Final Report

a. Federal Agency	Department of Energy	
b. Award Number	DE-EE0008394	
c. Project Title	Supercritical Treatment Technology for Water Purification	
d. Principal Investigator	Michael Mann Executive Director michael.mann@und.edu 701-777-3852	
e. Business Contact	Jamie Mitzel Grants and Contracts Administrator jamie.mitzel@und.edu 701-777-4146	
f. Submission Date	February 29, 2020	
g. DUNS Number	10-228-0781	
h. Recipient Organization	University of North Dakota	
i. Project Period	**Start:** Oct 1, 2018	**End:** Dec 31, 2019
j. Reporting Period	**Start:** Oct 1, 2018	**End:** Dec 31, 2019
k. Report Term or Frequency	Annual	
l. Submitting Official Signature		

MAJOR GOALS & OBJECTIVES

This project develops the Supercritical Water Extraction – Enhanced Targeted Recovery (SWEETR™) technology, a novel desalination process for treating hypersaline brines. The overall objective is to demonstrate the technical and economic feasibility of an innovative, energy efficient, and robust supercritical desalination technology to treat hypersaline solutions and separating saltwater into a pure water stream and valuable recovered solids, resulting in zero liquid discharge (ZLD). The proposed technology, focuses on innovative methods of applying supercritical water to treat highly concentrated brine solutions without incurring a high energy penalty. Integrating the technology with solar energy reduces the energy cost for the system.

Supercritical Water Extraction – Enhanced Targeted Recovery (SWEETR™) technology, applies the principle of "ultra-low salt solubility" in supercritical water to the treatment of high salinity brine and produced waters. One of the key innovations of our technology is the bulk fluid remains subcritical, minimizing energy requirements for treatment.

Table 1 presents the tasks, metrics, success value, and assessment tools for Budget Period 1 scope of work. As will be discussed in subsequent portions, sufficient progress was made on all milestones to achieve the proposed success values.

Table 1. Budget Period 1 Milestones and Assessment Criteria

Task	Task Description	Metric	Success Value	Assessment Tool
1	Update project milestones, SOPO, and critical path	PMP submitted	PMP accepted by EERE Federal Project Manager	Acceptance of PMP by EERE FPM
2	Perform initial technology and economic feasibility study	TEA submitted and accepted by EERE FPM	Design and performance criteria quantified and ranked based upon the contribution of each parameter to the cost of water treatment. A range of parameters required to meet the target of <$1.50 / m3 will be established.	Class V cost estimate developed in accordance to AACE International Standards - accuracy -20% to +100%. Sensitivity analysis performed on key variables over expected range of operation.
3	Modification and upgrade of laboratory-scale experimental equipment	Lab-scale equipment fully operational at specified design conditions	Ability to handle brine flow rates up to 30 ml/min, 300 bar, and 450 C temperature and ability to measure effluent TDS, propensity to scale, and relative corrosion.	The equipment will be tested to ensure it can reach the design conditions and measure the outcomes of interest with +-25% accuracy.

4	Evaluate the effect of temperature and pressure on solubility and solids separation	Relationship between solubility of salts and operating conditions developed	Pressure-temperature-solubility relationship mapped for region of interest	Measure the TDS levels in the effluent stream as a function of temperature (350 to 450 C), pressure (240 and 280 bar), and salinity level (3% to 15%)
		The TDS of the exit stream leaving the supercritical reactor	< 40,000 mg/L TDS	TDS analysis of effluent from the various test conditions

Budget Period 1 Go/No-Go Decision Point: A range of design and operating targets including temperature, pressure, feed-rate, and pretreatment options are identified where the SWEETR™ technology is technically and economically feasible. The laboratory-scale testing will develop a temperature/pressure vs. solubility map demonstrating the ability to produce clean product water quality of about 40,000 mg/L TDS or lower for a range of inlet water salinity and process conditions.

This project received a No-Go decision. Therefore this final project reports covers only those results from Budget Period 1.

1. PROJECT RESULTS AND DISCUSSION

1.1. Task 1: Project Management and Reporting

The purpose of this task was coordination and planning of the Project with DOE-EERE and Project Participants. The Project Management plan was updated as a part of the contract negotiation and the final project milestones and deliverables included in the contract package. Quarterly reports have been submitted for the first four quarters and the project team participated in the 2019 SETO CSP Program Summit.

Regular team meetings were held with team members. Envergex LLC had an on-site team at UND and interacts on a daily basis. Creedence Energy Services is located in Western North Dakota, and is on site at UND about once per quarter and corresponds with the team via phone on a regular basis. The Doosan team is located in Korea and correspondence with those team members is via email and phone conference.

1.2. Task 2: Initial Technology and Economic Feasibility Study

Preliminary Market Analysis: *SWEETR™ (Supercritical Water Extraction – Enhanced Targeted Recovery)* technology is an innovative, efficient, and economical approach for the separation of contaminated saltwater into *usable water* AND *valuable recovered solids*, and for the *destruction of organics* in the wastewater, resulting in *zero waste liquid discharge* (ZLD). For the produced water (PW) treatment, which is our initial target market, the *value created* with our technology *is more than $8/m^3* when considering the

value of the freshwater produced, sale of recoverable salts, and mitigation of current disposal costs. The cost for the alternative – disposal in regulated wells is about \$6/m^3. This provides an economically viable path for the developing this technology, because we can afford the higher initial costs for early generation of the product.

The market for SWEETR™ technology is the treatment of high salinity brines. Highly concentrated salt brine effluents are generated from a variety of sources, including seawater and brackish water desalination processes, produced water from fossil fuel (oil and gas) production, power plant scrubber and cooling tower blowdowns, and coal and metal ore mine tailing leachate. We focus on two of these markets: treatment of produced water (PW) from oil and gas operation, as the initial focus, and desalination of brines from existing desalination process, over the longer-term.

Produced Water Treatment: A near-term opportunity for SWEETR™ is the treatment of produced water (PW) from unconventional (shale) oil and gas production because of the high cost for its disposal. Oil fields, natural gas wells, and coalbed methane all generate large quantities of produced water with high Total Dissolved Solids (TDS) [2]. PW includes formation water (trapped underground) and injection water that are extracted together with the oil and gas during production. Composition of the produced water stream is complex. Major constituents of PW are: salts, organics including hydrocarbons (e.g. benzene, phenol, acetic acid), and additives used in fracturing and well operations (e.g. biocides, corrosion inhibitors, gelling agents). Formation water samples are generally very saline; for example PW from the Bakken formation has TDS in the ranges of 100,000 mg/L to as high as 350,000 mg/L [3]. The high salinity of the PW and its organic content limits its reuse, and requires treatment or transportation and deep injection into special disposal wells, adding several percentage points to the cost of oil and gas production. Transportation and disposal costs are high and significant (~\$2-10/m^3). Disposal costs in the Williston Basin of ND are reported to be approximately \$ 1.00/bbl. (\$6.3/m^3) [4]. As another example, in the case of natural gas production from the Marcellus shale in Pennsylvania, the wastewater is trucked to Ohio for disposal [5]. Treatment of the PW on-site by SWEETR™ technology would eliminate disposal cost, minimize environmental liability, as well as reduce freshwater demand.

Quantities of produced water are increasing dramatically. In 2010, considering the global production of oil and related water, the water to oil ratio (WOR) was about 3:1; however, by 2025, due to ageing wells, the WOR is expected to reach an average of 12:1 for onshore crude oil resources [1]. This reinforces the dramatic growth opportunity for PW management.

Focusing on the US oil and gas industry, EIA estimates U.S. crude oil production averaged 12.3 million bbl/day in 2019, highest on record [6]. EIA estimates continued growth to 2020 to 13 million bbl/d, with unconventional oil contributing more than 80% of production, and approximating 8% compound annual growth ratio (CAGR). Oil formations in the US include the Bakken (~12% of US production), Eagle Ford (~11%), Permian (37%), and Niobrara (22%). In addition to oil production, EIA forecasted that U.S. shale gas production averaged a record high of 83.3 billion cubic feet per day (Bcf/d) in 2018 and that it will increase to 92.2 Bcf/d in 2020.

Assuming a water-to-oil ratio (WOR) of 3:1 [1], unconventional oil drilling is estimated to produce about 5 million m^3/day of high TDS-produced water (PW). Similarly, using the Barnett Shale as an example, where PW to gas ratio was estimated by Rosenblum et. al. [7] at 4 m^3/million MCF, PW quantities from US unconventional gas wells are estimated to be about 0.4 million m^3/day. Increases in the Appalachia and Permian regions drive the forecast growth for shale gas. Both unconventional (shale) oil and gas represent a large growth market for water treatment with good economics.

The cost of treatment of high-TDS water with zero liquid discharge was estimated to be about ~ \$7/m^3 using a current alternative of lined evaporative ponds [1]. These unit costs are similar to that for disposal of PW in the Bakken (see above). If approximately 10 percent of the above high-saline water resources are addressed by SWEETR™, it would result in a potential early market opportunity of approximately \$2 billion annually, using a similar unit cost benchmark.

Desalination: A longer-term market for SWEETR™ is the desalination of discharge brines from existing desalination process. Currently, all commercial desalination process separate intake water into two different streams – a freshwater stream (product water) and a concentrate waste stream (brine). The disposal of effluent produced in the desalination process is a particular environmental concern and a potential liability and a major technical and economic challenge [8]. The brine effluents can cut levels of oxygen in seawater near desalination plants with "profound impacts" on shellfish, crabs and other creatures on the seabed, leading to "ecological effects observable throughout the food chain. The International Desalination Association reported that, as of 2017, there were greater than 19,000 desalination plants worldwide, with a total production capacity greater than 92.5 million m^3/day of fresh water [10]. Annual market growth for installation of new desalination plants is estimated at 5 million m^3/day capacity.

Membrane technologies continue to dominate the desalination market accounting for greater than 90 percent of the contracted capacity, while thermal processes account for the remainder [11]. The waste brine effluents from membrane and thermal desalination plants are a major source of brine (140 million m^3/day or 34.8 billion m^3/y) with high levels of total dissolved solids (TDS~70,000 ppm) [12]. Recovery ratios of clean water (to inlet seawater) are about 0.4 for membrane processes and only 0.2 for thermal processes. Assuming a mean unit cost of \$ 1/m^3 [4] for desalination, which would be a long-term cost target for our technology, results in a \$35 billion market that is growing 5 percent annually.

A key objective and advantage of the SWEETR™ technology is the elimination of brine discharge and production of only clean water and solid salts. Another advantage would be a reduction in the capital expenditures related to intake and brine discharge and pretreatment, which represent almost 40 percent of the overall capital cost for a RO plant and even higher for thermal desalination [13].

Considering both the short-term application to treat produced water from shale oil and gas wells (higher unit price) and the longer-term application to treat desalination plant discharges, the market size for SWEETR™ is large, and considering the growth in desalination and depletion of freshwater sources, the market is expected to continue to grow even more rapidly.

Customers: Customers and applications for our SWEETR™ technology are diverse and global. They include facilities that generate highly concentrated salt brine effluents, including seawater desalination processes, which take in water with a certain salt concentration (e.g. 35,000 ppm) and split it into clean water and a discard brine (e.g. 70,000 ppm salt), oil and gas operations (produced water returned with the oil has very high salinity ranging from 100,000 to 350,000 ppm salt), coal and metal ore mining operations, power plants (scrubber and cooling tower blowdown). In addition to these end customers, our direct customers would be equipment and service suppliers and technology providers to these facilities.

Our initial application is for treating produced water from oil and gas operations, with focus on unconventional (shale) oil and gas wells. We have reached out to oil and gas producers like ExxonMobil in Houston, TX who have expressed a strong interest in our technology. Our discussions indicate that PW disposal is an increasing challenge that is a significant line item in the cost ledger for oil and gas production at several locations. This is due to lack of accessible wastewater disposal sites in close proximity. Furthermore, the organic component(s) in the produced water, in particular, is a potential long-term environmental liability.

Our project partners represent two different options on the commercialization pathway. Creedence Energy Services[1], headquartered in Minot, ND, provides chemical treatments and solutions to prevent scaling problems for oil and gas operators in the Williston Basin. The SWEETR™ technology has the potential of generating salts and other chemicals from high-TDS brine processing. This is an additional market opportunity for Creedence's business, and their distribution network would aid in the marketing of recovered salts and other minerals. Doosan Heavy Industries[2] (DHI), a leading global supplier of water treatment systems is exploring new growth engines in water treatment and has expressed a very strong interest in our approach as indicated by their participation in this project.

In addition to oil and gas field applications, our technology addresses a critical drawback for current and future desalination plants – avoiding discharge of hypersaline residuals. Demand for desalination worldwide is increasing rapidly. Most coastal communities including those in Middle East, India, Australia, USA, and Africa face high water stress imposed by local population growth. According to Doosan, combining SWEETR™ technology with existing desalination approaches can remove a current handicap of retentate discharge. Ensuring cost-effective zero liquid discharge as well as valuable salt recovery would make desalination more economical and enable a broader market penetration.

Based upon discussions with industry in the region, the preliminary design presents two different scenarios which reflect the impact of economies of scale. The preferred design is based upon smaller units designed to service a single well pad. The base system is sized to treat 2000 bbls/day of produced water (100,000 m^3/yr). A larger, centralized

[1] http://www.creedence-energy.com

[2] http://www.doosanheavy.com/en/intro/randd/water/

system of 20,000 bbls/day (1,000,000 m^3/yr) is also considered. The target inlet TDS for the design, based upon the water quality in the Bakken, is 200,000 to 300,000 mg/L.

Process Flow: The basic design for the process is shown in the block flow diagram as Figure 1. A process flow diagram was developed using Aspen Plus V.10. This provided the basis for the Technology and Economic Assessment (TEA). The process flow diagram was based upon the concept proposed in the initial project proposal and included updates based upon what has been learned in the companion STTR project (see summary in Task 4 "Update on the State of the Art" section of this application). This TEA was meant only as a preliminary assessment to determine major cost components with the intent of prioritizing research direction. The final, more definitive and complete TEA was planned as a separate task for Budget Period 3.

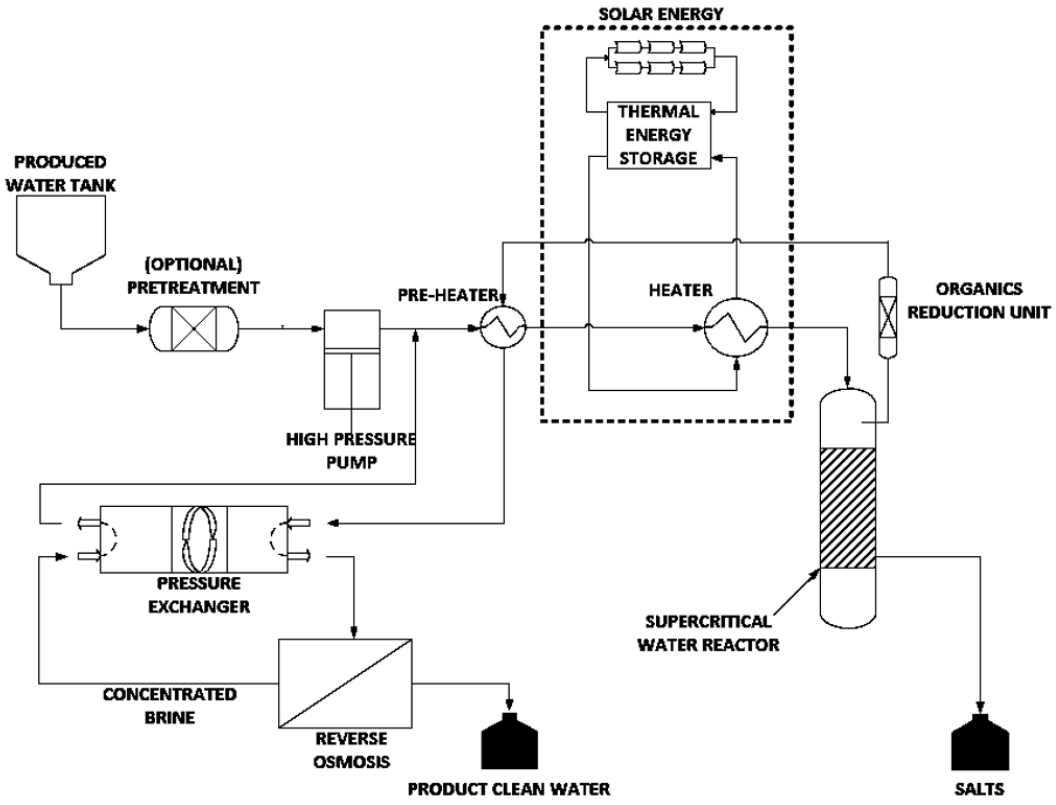

Figure 1. Block flow diagram of SWEETR technology.

A material balance for the 1000 bbl/day system has been developed as a baseline for a small-sized system to serve a single well pad. The process as modeled does not include any pretreatments steps. The necessity for pretreatment would have been determined in the later part of this project. The process is shown with the brine directly entering a high pressure pump to increase its pressure to the operating pressure for the reactor. Under the proposed scenario, the preheater will cross exchange with the recycled stream to recover the thermal energy from that stream. The now-heated brine stream will be sent

into the solar heater where the temperature will be increased to within a few degrees of the process temperature. The final temperature rise will occur in the supercritical reactor.

The solar power heater included in the process flow diagram is black boxed at this point with additional design to be done in conjunction with Doosan. A number of alternatives have been discussed. The proposed approach would use solar energy to heat a molten salt (Dynalene) to indirectly heat the reactor. The operating temperatures of the salt are in the right range for what we hope to accomplish. This scenario was used for estimating the CAPEX and OPEX in the preliminary TEA. We also looked at other options including a thermal fluid such as Dowtherm (may have too low of operating temperature) and using PV along with electric heaters (concerned about the low conversation efficiency of solar energy to electricity).

After solar heating, the brine is sent to the supercritical (SC) reactor where it will be combined with air to destroy the organics and to achieve the temperature required to facilitate solids precipitation. The air will be supplied using a multi-stage compressor to achieve the required process pressure.

The target exit brine concentration from the SC reactor is 40,000 mg/L TDS. As discussed in the original proposal, this was chosen as a level that can be accepted by reverse osmosis (RO) while allowing the supercritical process to be performed at “relatively mild” conditions thereby reducing the overall cost of the system. However, preliminary experimental work performed during Task 4 indicates that the energy penalty may not be as large as originally perceived, and future work will also target near complete removal of TDS.

A solids separation stage will occur to remove any suspended solids in the treated brine. Once the solids are removed, brine will be sent to a stream splitter. As originally conceived, under typical operation, the splitter will send all of the brine into the recycle line and ultimately to the RO system. A gas removal stage is included to vent any excess oxidant and any gaseous products formed from the destruction of the organics. The splitter would divert the treated brine only in necessary cases when either the brine cannot be recycled into the preheater (i.e. maintenance or process upset) or for cases where the brine concentration from the supercritical reactor meets the customer’s needs. As will be discussed later in the report, results from this work show the cost of recycle to be excessively high for the benefits received. Therefore, the final process likely will not include recycle as an option.

Following the recycle stream across the preheater, the next unit operation is a pressure exchanger. The goal is to decrease the pressure to match the inlet requirements of the RO unit and then increase the pressure back to the SC process condition. After the initial pressure reduction, a cooler may be required to bring the stream down to levels to the required RO inlet specifications. The RO unit was designed for a retentate concentration of 80,000 TDS with a permeate stream of 500-1000 TDS clean water. The final design will be optimized by Doosan. The retentate from the RO unit is brought back to SC pressure with the pressure exchanger and mixed together with the inlet brine, thereby facilitating the zero discharge of brine waters. The clean water can be produced to match specifications of the end user/market.

A detailed mass balance for the entire process has been performed for the case of 1000 bbl/day (160 m^3/day or 50,000 m^3/year at an 85% capacity factor). These mass flows were used by Doosan as they performed the preliminary equipment sizing and cost analysis.

CAPEX Methodology: Engineering rules of thumb were used for cost analysis. An Excel spreadsheet was constructed to provide flexibility in exploring the impacts of materials of construction and other critical assumptions that may drive the process development. Some of the underlying assumptions and critical results are summarized here.

One of the critical components for this design is the heat exchanger that will be used to recover the heat from the supercritical reactor and to preheat the brine water entering the supercritical reactor. A U-tube type is used for heat exchanger's head. Material factors were varied depending on the pressure and temperature. An Excel file is programmed to allow selection of different tube and shell materials. Material factors for tube and shell are shown in Table 2 and underscore the importance of understanding the level of corrosion to be expected for each metallurgy and not over designing the system. The most expensive material is titanium/titanium and the cheapest is carbon steel/carbon steel for tube/shell. The difference between them is about a factor of 11x as construction cost.

Table 2. Material of Construction Factors for Heat Exchanger.

Tube	Shell	a	b	Material factors
Carbon steel	Carbon steel	0.00	0.00	1.00
Carbon steel	Brass	1.08	0.05	2.25
Carbon steel	Stainless steel	1.75	0.13	3.24
Carbon steel	Monel	2.10	0.13	3.59
Carbon steel	Titanium	5.20	0.16	6.83
Carbon steel	Cr-Mo steel	1.55	0.05	2.72
Cr-Mo steel	Cr-Mo steel	1.70	0.07	2.94
Stainless steel	Stainless steel	2.70	0.07	3.94
Monel	Monel	3.30	0.08	4.58
Titanium	Titanium	9.60	0.06	10.80

For the design of these heat exchangers, a tube outside surface area of 198 m^2 is estimated, with a shell-inside pressure of 20000 kPa. Tube length should be 8 m with 20 paths, with a 1.0 m/s velocity in the tube. It was assumed that the liquids on both sides of the heat exchanger were subcritical.

Pumps were designed according to the flow rate and pump head. Centrifugal pumps are used for this system. Material of construction factors for centrifugal pumps are shown in Table 3.

Table 3. Material of Construction Factor for Centrifugal Pumps.

Materials of construction	Material factors
Cast iron	1.00
Ductile iron	1.15
Cast steel	1.35

Bronze	1.90
Stainless stell	2.00
Hastelloy C	2.95
Monel	3.30
Nickel	3.50
Titanium	9.70

The basis for the reverse osmosis (RO) system is calculated by ROSA, which is commercially used for membrane system design. System feed conditions are as follows: feed flow rate is 300 m^3/day, feed pressure is 57.01 bar, total membrane active area is 490 m^2, feed temperature is 30℃, and feed TDS is 40,000 mg/L. TDS includes only sodium and chloride. Six membrane elements are used for this system. Table 4 shows the conditions for the RO system.

Table 4. Reverse osmosis (RO) system condition.

Feed Flow to Stage 1	300.00	m^3/d
Raw Water Flow to System	300.00	m^3/d
Feed Pressure	57.01	bar
Flow Factor	0.85	
Chem. Dose (100% H_2SO_4)	0.00	mg/l
Total Active Area	490.51	m2
Water Classification: Seawater with Conventional pretreatment, SDI < 5		
Pass 1 Permeate Flow	114.01	m^3/d
Pass 1 Recovery	38.00	%
Feed Temperature	30.00	C
Feed TDS	40000.01	mg/l
Number of Elements	12	
Average Pass 1 Flux	9.68	lmh
Osmotic pressure		
Feed	32.26	bar
Concentrate	53.35	bar
Average	42.80	bar
Average NDP	13.88	bar
Power	24.75	kW
Specific Energy	5.21	kWh/m^3

The supercritical reactor was sized to provide the desired residence time (the required residence was to be determined as a part of Task 5 in Budget Period 2 and may have a notable impact on the CAPEX). Carbon steel was used as the basis for the supercritical reactor material, with a material factor for nickel cladding applied to account for anticipated materials of construction. It is recognized that a higher grade of material and/or cladding may be required and the final material selection will need to be determined as a part of the experimental work associated with this project.

The cost of the concentrated solar panel and heat exchange system was estimated using values reported in an NREL report. In their report a total cost of a CSP system was estimated as \$5800/kW_e. For our estimation, this value was adjusted be removing the percentage of those costs associated with the electrical generation portion of the system where those percentages were obtained from published literature values. The cost used in our estimate was \$4970/kW_e. The cost in dollars per kilowatt thermal (\$/kW_{th}) was calculated to at \$1242/kW_{th}. This value was determined by factoring in a 25% efficiency on the conversion from thermal energy to electrical energy in a CSP. Thus the thermal cost (\$/kW_{th}) will be four times less the electric generation price. The value for this subsystem will be updated during the final TEA in budget period 3 based upon the heat duty requirements determined from the experimental work and the system integration scheme developed during the final design.

CAPEX Results: Depending on the materials chosen for the system, the CAPEX varies significantly, underscoring the importance of fully understanding the corrosion rates associated with this system. A number of comparisons were made using various materials of construction to set a realistic range of CAPEX for the system. Based upon the preliminary work performed, the capital costs for the system as proposed was estimated at approximately \$5.5 million if stainless steel is used for the pumps, monel/monel for the heat exchanger, and nickel-cladded steel for the supercritical reactor (see Table 5 for a cost estimate for this scenario), and a commercial air compressor is used: HK500, and pressure with a pressure of 210 bar.

Table 5. Capital Costs Estimate using Stainless Steel Pump, Monel/Monel Heat Exchanger, and Nickel-Clad Steel Reactor.

	Total	Pump 1	Pump 2	Heat Exchanger	SC Reactor	Air Compressor	Pressure Exchanger	CSP	RO	Magnetic Separation
Capital Costs	**5,537,890**	**148,943**	**148,367**	**547,799**	**3,241,598**	**121,664**	**172,356**	**497,000**	**565,230**	**94,933**
Total CP	**2,280,660**	52,702	52,498	193,832	1,147,002	43,049	60,986	497,000	200,000	33,591
Equipment Cost	**2,521,454**	59,817	59,585	220,000	1,301,847	48,861	69,219	-	227,000	38,126
Purchased Equipment Installation	**364,402**	10,767	10,725	39,600	234,332	8,795	12,459	-	40,860	6,863
EC & I (Including Services)	**364,402**	10,767	10,725	39,600	234,332	8,795	12,459	-	40,860	6,863
Piping	**404,891**	11,963	11,917	44,000	260,369	9,772	13,844	-	45,400	7,625
Manual Valves	**303,668**	8,972	8,938	33,000	195,277	7,329	10,383	-	34,050	5,719
Insulation and Painting	**101,223**	2,991	2,979	11,000	65,092	2,443	3,461	-	11,350	1,906
Site Improvement	**364,402**	10,767	10,725	39,600	234,332	8,795	12,459	-	40,860	6,863
Service Facilities (Including Installation)	**121,467**	3,589	3,575	13,200	78,111	2,932	4,153	-	13,620	2,288
Steelwork	**1,010,223**	2,991	2,979	11,000	65,092	2,443	3,461	-	11,350	1,906
General Facilities Capital	**202,445**	5,982	5,959	22,000	130,185	4,886	6,922	-	22,700	3,813
Engineering & Home Office Fees	**141,712**	4,187	4,171	15,400	91,129	3,420	4,845	-	15,890	2,669
Project Contingency Cost	**303,668**	8,938	8,938	33,000	195,277	7,329	10,383	-	34,050	5,719
Process Contingency Cost	**202,445**	5,959	5,959	22,000	130,185	4,886	6,922	-	22,700	3,813
Royalty Fees	**40,489**	1,196	1,192	4,400	26,037	977	1,384	-	4,540	763

The above is considered a technically conservative design, where all of the selected materials are expected to have good lifetime under the proposed operating conditions. If the system used carbon steel for as the basis, the capital cost will be approximately \$2.0 M. While this case is unrealistic due to corrosion concerns, it can be used to show the lower target with regard to capital costs. Material selection is big factor in determining the system design cost and is being carefully decided for the system. A detailed comparison of first cost versus replacement costs/time will be evaluated as a part of this study.

To highlight the impact of material selection on capital cost, detailed cost differences are shown in Table 6 for pumps. Cast iron is used as the basis. Titanium is the most

expensive and durable for the system. A titanium pump is 9.7 times more expensive than cast iron.

Table 6. Pump Costs as a Function of Material of Construction.

Materials	Factors	Pump 1 ($)	Pump 2 ($)
Cast iron	1.00	74,472	74,184
Ductile iron	1.15	85,642	85,311
Cast steel	1.35	100,537	100,148
Bronze	1.90	141,496	140,949
Stainless steel	2.00	148,943	148,367
Hastelloy C	2.95	219,691	218,842
Monel	3.30	245,756	244,806
Nickel	3.50	260,650	259,643
Titanium	9.70	722,374	719,582

Detailed cost differences for the heat exchanger are shown in Table 7. Carbon steel/carbon steel is the baseline for shell and tube. Comparing to the carbon steel and carbon steel, the titanium and titanium cost are 9.6 times expensive.

Table 7. Heat Exchanger Costs as a Function of Material of Construction.

Material of Construction Shell/Tube	a	b	Factors	Heat Exchanger ($)
Carbon steel/carbon steel	0.00	0.00	1.00	197,548
Carbon steel/brass	1.08	0.05	2.25	443,517
Carbon steel/stainless steel	1.75	0.13	3.24	639,626
Carbon steel/Monel	2.10	0.13	3.59	708,768
Carbon steel/titanium	5.20	0.16	6.83	1,349,390
Carbon steel/Cr-Mo steel	1.55	0.05	2.72	536,364
Cr-Mo steel/Cr-Mo steel	1.70	0.07	2.94	580,504
Stainless steel/stainless steel	2.70	0.07	3.94	778,053
Monel/Monel	3.30	0.08	4.58	904,175
Titanium/Titanium	9.60	0.06	10.80	2,133,770

Implications of CAPEX Analysis: To help guide the development of the project, the projected cost of each component was compared for the base case to determine the interaction between capital and operating costs, and the impact of including various auxiliary pieces of equipment. Experimental data generated during the first phase of the work was also used to determine the optimal equipment orientation. The Doosan capital cost model was adjusted to evaluate the overall magnitude of these changes on estimated capital costs. For the revised case, using stainless steel as the material of construction for the primary pump, monel as the material of construction for the heat exchanger, and nickel-clad for the super critical reactor, the projected capital cost for the system is $3.4

million (Table 8). This is a 40% reduction from the $5.5 million projected cost for the base case.

Table 8. Capital Costs Comparison between Base-case and Revised-case.

	Base[2]	Revised[3]
Throughput (m^3/year)	**58,400**	**58,400**
Pump 1	$149,000	$149,000
Pump 2	$148,000	-
Heat Exchanger	$548,000	$433,000
SC Reactor	$3,240,000	$2,100,000
Air Compressor	$122,000	$122,000
Pressure Exchanger	$172,000	-
CSP	$497,000	$497,000
Reverse Osmosis	$565,000	-
Solids Separator	$95,000	$95,000
Total Capital Cost	**$5,540,000**	**$3,400,000**
Annualized CAPEX[1], $/$m^3$	8.00	4.91

[1]CAPEX annualized to 20 years at 5%
[2]Base cases assumes stainless steel pump, monel/monel heat exchanger, and nickel-clad steel reactor.
[3]Revised case simple once through system. Assumes stainless steel pump, monel/monel heat exchanger, and nickel-clad steel reactor.

On a cost per volume water treated, the capital cost for the two scenarios are $8.00/$m^3$ and $4.91/$m^3$, respectively for a small-scale single well pad system. These are higher than the preliminary capital cost estimates, however, they are still within the range that make the less than $1.50/$m^3$ a viable target when considering the entire value proposition (e.g. wastewater disposal credits) of the proposed technology. These numbers will guide the development individual unit operations, and also to evaluate different implementation strategies. For example, consideration of the option of a centralized versus well pad location to take advantage of economies of scale is discussed in the OPEX discussion below.

OPEX / Methods: The operating costs associated with the system were broken down into four categories, energy cost for pumping and compression, energy cost for heat input (CSP), maintenance, and labor. An operating factor of 85% was considered when calculating the OPEX. The energy cost for pumping and compression was determined by taking the electrical demand, determined from Aspen Plus simulations, and multiplying by an electricity cost of $0.075/kW-hr. CSP costs (i.e. energy cost for the heat input) were determined by using an energy demand of 225 MJ/m^3-feed and multiplying by the feed flowrate and the CSP energy cost of $0.025/kW-hr. This cost of thermal energy is the predicted O&M cost of a CSP system as reported from the International Renewable Energy Agency (IREA) report and is used to as a way to capture the tradeoffs of higher removal efficiency versus energy input [14]. For the maintenance costs, a general assumption of 5% of capital cost per year in maintenance was utilized. Labor costs were

calculated using a loaded labor cost of $50/hour and multiplying by the number of man hours required. The number of man hours required for the 50,000 m^3/year was estimated to be on average 6 dedicated man hours per day. Therefore, a single operator could service multiple systems in a single shift. For the 1 million m^3/year system it was estimated that 64 man hours per day are required.

TEA Summary: A summary of the capital and operating costs and credits is presented in Table 9. The table compares two options, the "Revised" case presented in the CAPEX section and Table 8 at 58,400 m^3/yr. design capacity (single pad design) and a 20 times larger scale "Revised" case (centralized plant) to show the effects of scale. To determine the new capital cost for the larger size, the sixth-tenths rule was applied to the CAPEX. The total credits available include the sale of recovered salts at $25/ton, disposal cost mitigation, and the value of recovered freshwater.

Table 9. Summary of Primary Results from Preliminary TEA.

Costs in $/m^3	**Revised**	**Revised**
Throughput[a] (m^3/yr)	50,000	1,000,000
Capital Cost (20 years annualized at 5%)	4.91	1.51
Energy Cost (pump and compressor)[b]	1.24	0.69
Energy Cost (heat input)[c]	1.33	1.33
Maintenance[d]	2.91	0.90
Labor	2.21	1.18
Total Operating Cost	**12.60**	**5.61**
Sale of Recovered Sale[e] ($25/ton)	-5.28	-5.28
Disposal Cost Mitigation	-6.00	-6.00
Freshwater Value[f]	-3.00	-3.00
Total Credits	**-14.28**	**-14.28**
Net Cost of Treatment (Value Proposition)	**-1.68**	**-8.67**

[a]At an 85% operating factor
[b]Assumed Electric Cost of $0.075/kW-hr
[c]Assumed CSP costs of $0.025/kW-hr and demand of 225 MJ/m^3
[d]Maintenance assumed as 5% of total capital cost
[e]Salt recovered from feed stream of 200,000 TDS
[f]Water recovery equal to 80% of feed volume

Significant economies of scale can be realized in a centralized plant. As the final commercialization plan is developed, the implication of transportation costs for both scenarios will be considered.

As shown in Table 9 above both sizes of the revised system are able to achieve a value proposition less than $1.50/$m^3$, thereby meeting the stated goals of this original proposal. The negative value proposition represents potential income for the commercializing entity, with the significant credits available in this market making the treatment of brine from the oil and gas fields an ideal application for the first market penetration.

Task 3: Modification and Update of Laboratory Scale Experimental Set-up

An existing system that was designed and constructed for proof-of-concept testing for a separately funded DOE Phase I STTR (DE-SC0018523) the equipment was modified and upgraded for use in this project. The material for construction for the system was 316L stainless steel. The flow path is made mostly of Swagelok® fittings and tubing, with the main body of the reactor being supplied by High Pressure Equipment Co. Construction materials which are appropriately rated for the operating temperatures and pressures of the system. The setup consists of a high pressure pump (Eldex BBB-4). Electric ceramic heaters capable of reaching above 500°C are used to externally heat the preheater and reactor sections to achieve the desired temperature for operating conditions. Additional instrumentation was installed to measure more temperatures and pressures in critical areas of the flow path and reactor. The product streams are cooled in a heat exchanger and filtered prior to the back pressure regulator (BPR). Total Dissolved Salts (TDS) is measured at ambient pressure and temperature before the high pressure pump and after the BPR using two inline conductivity sensors (400VP-13) wired to a Rosemount™ 1056 Dual-Input Intelligent Analyzer sourced from Emerson. A 400 bar nitrogen gas bottle and high pressure gas regulator is used to set the regulating pressure of the BPR.

The reactor is designed to be modular with extra ports allowing for easy manipulation. Applications for these extra ports can be: more instrumentation/sensors (pressure transducers, thermocouples), salt removal, valves/drains, and a fitting with metal coupons for additional corrosion and scaling testing. Multiple thermocouples are added to the reactor to verify the establishment of a temperature gradient. The system was designed to be capable of isolating the reactor from the upstream and downstream components to facilitate additional data/sample collections. To preserve the deposited solid samples in the reactor zone, high pressure N_2 gas will be used to blowdown and empty the system of the liquid solution. Equipment was designed to blow down the system in three isolated sections: Upstream Reactor, Reactor, and Downstream Reactor. The liquid samples from these individual sections can then be retained separately and analyzed.

The experimental set-up is shown in Figure 2. As stated previously, the reactor design is modular, which allows the reactor to be operated in various configurations.

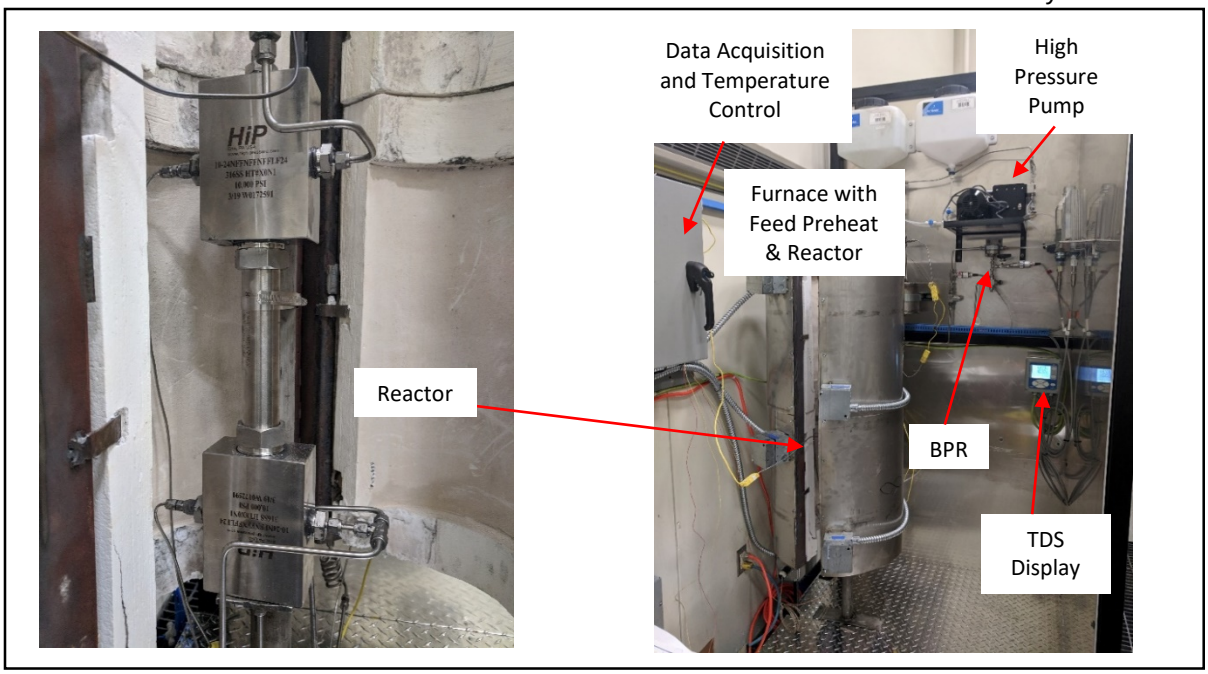

Figure 2. Experimental equipment set-up.

1.3. Task 4: Evaluation of Effect of Temperature and Pressure on Solubility and Solids Separation

Summary of Results from STTR Project: The basis of the current equipment design and set up was derived from proof-of-concept experimental work done through a separately funded DOE Phase I STTR (DE-SC0018523). The Phase I STTR project was developed as a proof-of-concept study for the SWEETR™ technology. Results from the STTR project provide a foundation for and guide the experimental activities in the current project.

The equipment in the current project has been upgraded for extended testing capabilities, and scale-up with larger volumes for solids collection and higher flow rates of feed solution.

The key conclusions from the STTR project are summarized below.

- For the NaCl–H_2O system, at pressures and temperatures near the critical value, a two-phase region is formed (one phase is water vapor with very low salts concentration in equilibrium with a second phase comprising concentrated brine, and at even higher temperatures, the second phase is a solid salt). We focus our operation near these pressure and temperature regions.
- Supercritical zones for salt precipitation were generated by heat addition. The degree of salt removal could be tuned by adjusting the local temperature.
- A substantial reduction in the organic component concentration in the effluent, with the possibility of near-complete organics removal was demonstrated.
- Test conditions also showed the potential for corrosion and scaling reduction.

Experimental Methodology:

Conductivity vs. Concentration Measurements: Feed solutions were prepared on a weight percent basis. This is the consistent method of preparation across supercritical water desalination thesis work done by Odu [15] and Hodes [16] for the higher concentration salts and is important as the correlation between TDS and conductivity (mS/cm) is not linear at higher concentrations. Preparing a 20 wt% sample with inputs of 200g NaCl and 800g water produced a total aqueous solution volume of 880ml. This matches closely with calculations done for measuring total volume of a solution after mixing solvents in aqueous solutions. The experimental density for the salt solution is 1.136 g/ml. This is within 0.9% error of the density handbook value for 20 wt% NaCl solutions - 1.147 g/ml [17]. According to these references, 20 wt% NaCl should produce a conductivity of 220-242 mS/cm pending on temperature [18, 19]. The bench-top lab conductivity measurements for the 20 wt% NaCl were ~240mS/cm. The inline conductivity sensors were then calibrated to match the experimentally verified conductivities.

Conductivity of a variety of NaCl concentrations were experimentally measured and graphed to be compared to literature to establish in-house correlation factors for conductivity vs. concentration. When corrected to 25°C, these values match literature [17-19] within 3% error. The correlation factor between conductivity and concentration can vary depending on the composition of the dissolved salts. The results of this literature review and experimental verification are presented in Figure 3 and Table 10.

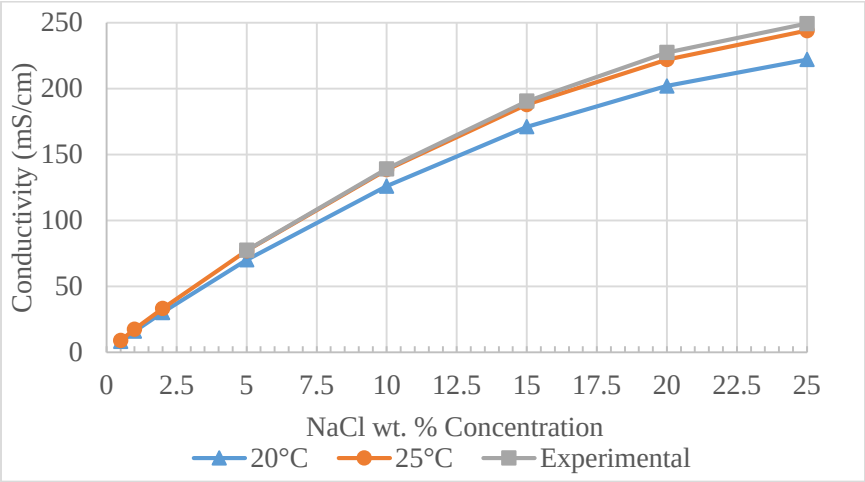

Figure 3. Concentration vs. Conductivity based on literature [17-19], coupled with experimental lab results.

Table 10. Concentration and conductivity with correction factor for NaCl.

Concentration (wt. %)	Conductivity At 20°C	Correction Factor 20°C	Conductivity At 25°C	Correction Factor 25°C
0.5	8.2	0.609	9.1	0.554
1	16	0.625	17.6	0.567
2	30.2	0.662	33.2	0.603

5	70.1	0.713	77.0	0.649
10	126	0.793	138.5	0.722
15	171	0.877	187.9	0.798
20	202	0.990	222.0	0.901
25	222	1.12	244	1.02

Mass Balance: The pump flow is set to 10 ml/min while flowing deionized water at pressure, 240 bar, before adding heat. Once at process conditions the flow-rate is again verified. The moment the inlet is changed from deionized water to feed solution, the exit effluent is collected. This bottle contains the DI water that remains in the system until salt water replaces it, assuming plug flow in the reactor. The moment the exit TDS increases above DI water levels, the exit effluent is collected separately. This collection represents the process TDS, which is used to help calculate the salt removal efficiency. Once a test is completed, at shutdown, the inlet feed is switched back to DI water - all while maintaining process conditions (temperature, pressure and flowrates). The TDS, volumes, and flow-rates are continued to be monitored. The effluent stream is collected while system is cooled and cleaned. This process helps close the mass balance better than taking every component apart, prevents plugging by always ensuring flow through the system, all while cleaning the system of solids. Mass balance of the salt removal from the feed stream ~95% recovery of the salt fed are typical.

Preliminary results: A feed stream of a preset salt concentration was preheated to 360°C where it entered the reactor. The stream was further heated to the desired bottom reactor set point through the addition of heat to the reactor. This increased the overall bulk temperature by approximately 20 to 80°C (heat input is a test variable). Testing was performed at 10 wt.% and 20 wt.% as it represents the general range of concentrations present in produced water samples. Temperatures and pressures were kept constant during each test. Experimental conditions tested are summarized in Table 11.

Table 11. Summary of test conditions.

Experiment	Salt Concentration	Pressure	Zone Temperature (°C)	Outlet Temperature (°C)	Flowrate (ml)
Condition-1	10 wt. % NaCl (100,000ppm)	~200 bar	23	23	10.0
Condition-2		~240 bar	361	359	13.8
Condition-3		~200 bar	380	380	9.0
Condition-4		~240 bar	400	390	9.7
Condition-5	20 wt. % NaCl (200,000ppm)	240 bar	361	363	12.5
Condition-6			385	370	10.0
Condition-7			415	407	11.5
Condition-8			420	410	12.5
Condition-9			427	412	10.7
Condition-10			435	400	9.6

Flow-rates were recorded and the exit conductivity monitored. The feed-bottle weights and volumes were tracked before and after each test. Results of the 10 wt% and 20 wt% are shown in Figure 4. The zero milliliter mark represents the point in time when the freshwater feed was changed to a salt-water feed. The first slight increase in conductivity is at the 150 ml/mark for most tests. Each test saw an increase in conductivity before the 300 ml (32-minute) mark. By the 280-330 ml fed range, the exit conductivity is reflective of a stream of salt solution that has passed through the reactor and is thought to be representative of steady state conditions.

The data Figure 4 shows a clear difference between the above 400°C tests and sub-400°C tests. The sub-400°C tests show an increase in conductivity immediately after the produced water begins to enter the reactor. This is reflected by the rise in conductivity in the 200 to 300 ml fed range (note the difference in the rise time between the three sub-400°C tests is due to slight variations in how the testing was performed). For the higher temperature tests, the outlet conductivity showed essentially complete removal of the salt (i.e. conductivity of ~0 at the 300 to 500 ml fed range). After a volume fed of over 500 ml of 20 wt% NaCl (100 grams of NaCl), the reactor starts to show signs of being volume limited for all but the highest temperature case as noted by the sudden increase in conductivity.

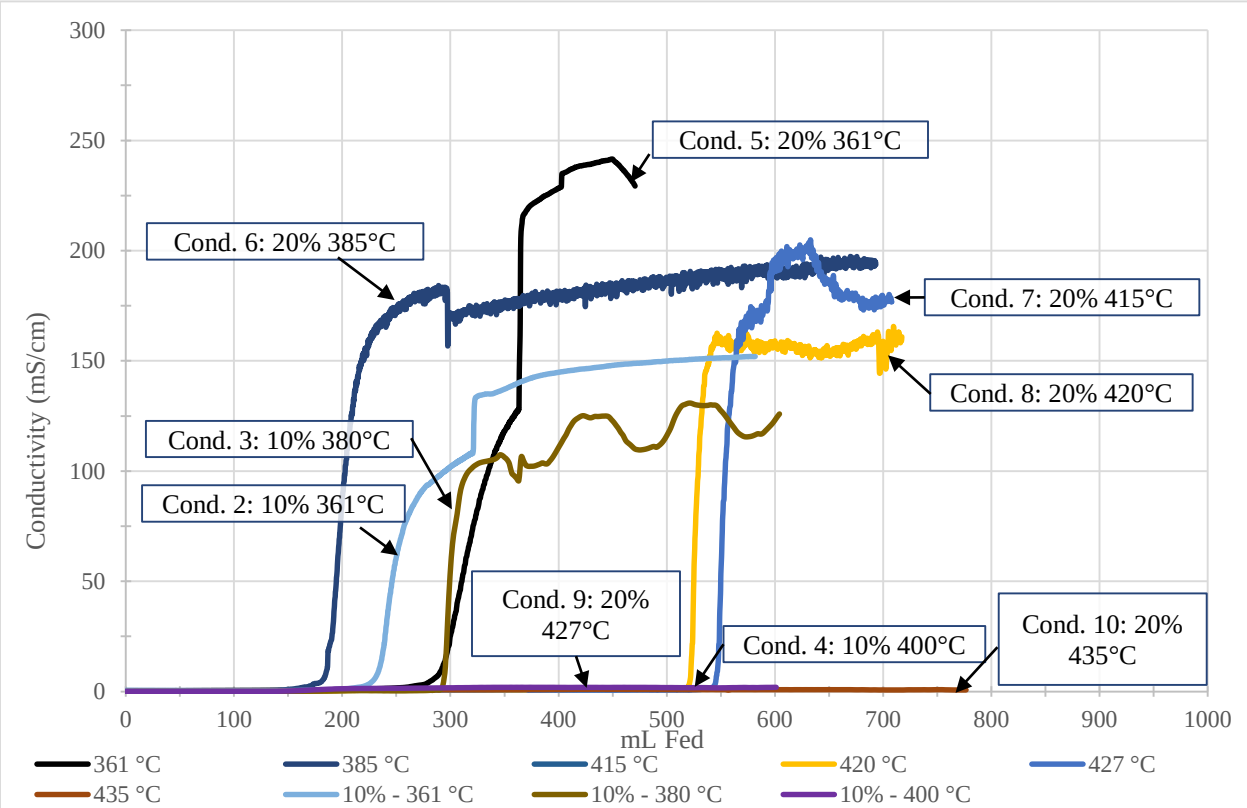

Figure 4. Outlet Conductivity vs. volume fed, 10 wt% and 20 wt% NaCl at varied temperatures.

Two baseline tests for conductivities measurements were ran at 360°C and 240 bar, one for 10 wt% NaCl and another for 20 wt% NaCl. These baseline conductivities are under conditions of 0% expected desalination. The exit conductivities by the 300 ml mark differ less than 1% when compared to their starting inlet concentrations (not shown in these graphs but monitored during the actual testing). These tests help establish that the reactor is operating under plug flow and there is minimal to no dilution.

Figure 5, shows three separate tests for a 10 wt% NaCl concentration. For the 361°C test, the exit salinity first increased at the 15 minute mark (150ml), before matching the starting salinity at the 30-35 minute mark (300-350 ml), showing no salt removal at this temperature. For the 380°C test, the exit salinity increased to a steady state value of approximately 120 mS/cm, representing a removal efficiency of ~ 10%. The test at 400°C showed no increase in salinity over the duration of the test, indicating a near 100% removal of salt for the entire test duration.

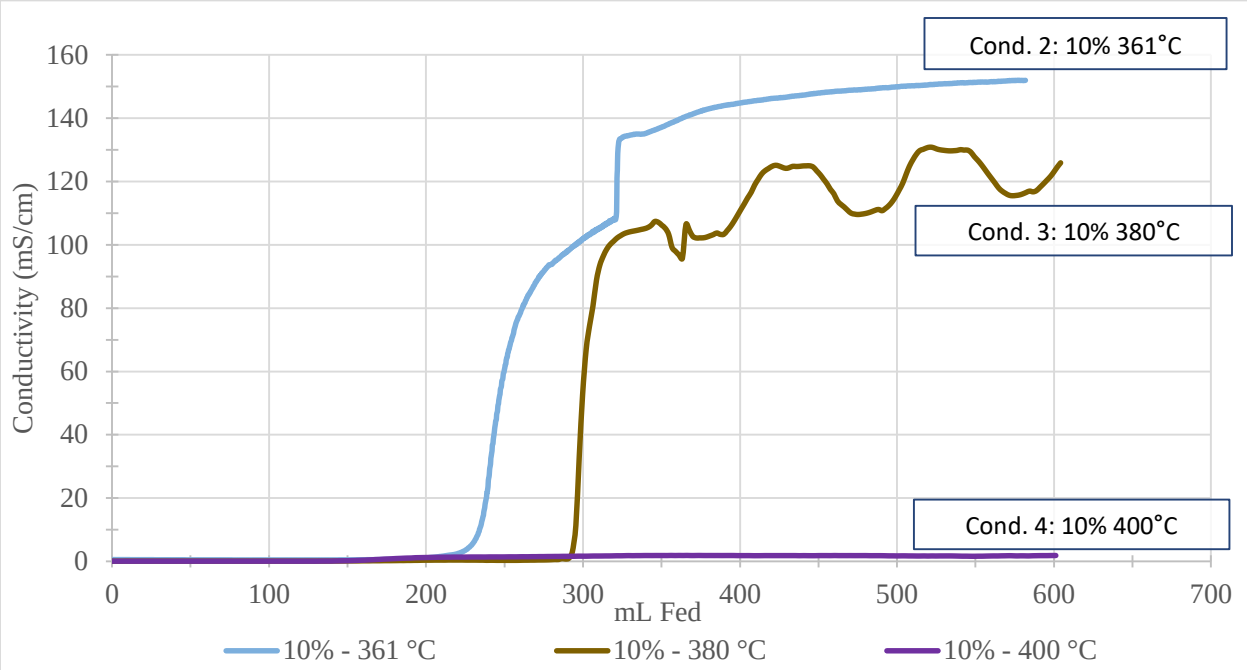

Figure 5. Conductivity vs. volume fed, 10 wt% NaCl Concentration.

During the first set of tests the temperature profiles indicated a rather high heat loss through the bottom of the reactor. Modifications included raising the reactor higher into the ceramic heaters and improving the insulation. The 20 wt% tests were performed with the improved temperature control.

Figure 6 shows the results from the six tests performed with the 20 wt% salt. The four tests above 400°C show 100% desalination up until the 500 ml mark. This is the point where the volume of salt in the lower reactor reaches capacity and the overall desalination efficiency decreases. The two tests below 400°C show minimal desalination with no salt reduction seen at 361°C and 27% reduction for the 385°C test.

The data set indicates that for all cases, salt brine had passed through the reactor and to the outlet conductivity sensor by the 300 ml mark for all tests. The overall desalination/salt removal percentages for each condition are shown in Table 12 as well as illustrated in Figure 7 and Figure 8. At temperatures below supercritical there is very little salt dropout. As temperature increase above the supercritical point, the salt dropout increases, approaching to 100% of the salt captured when exceeding 400°C.

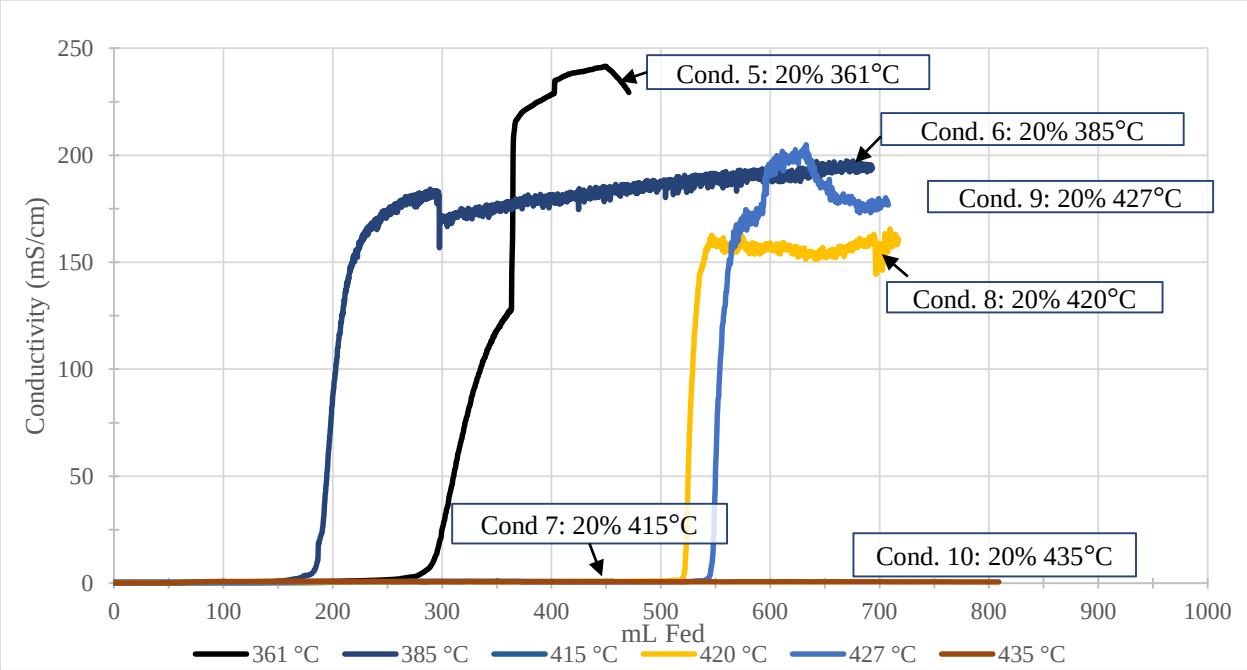

Figure 6. Conductivity vs. Volume fed, 20 wt. % concentration.

Table 12. Summary of results from effluent analysis.

Salt Concentration	Inlet Temperature (°C)	Inlet Conductivity (mS/cm)	Inlet TDS (ppm)	Outlet Conductivity (mS/cm)	Outlet TDS (ppm)	Removal Percentage (%)
10 wt. % NaCl (100,000ppm)	23	135	98000	135	97000	1.0
	361	153	110000	152	109000	0.9
	380	135	97000	121	87000	10.3
	400	138	99000	1.2	840	99.3
20 wt. % NaCl (200,000ppm)	361	228	205000	228	205000	0
	385	229	206000	190	150000	27.2
	415	227	204000	0.7	490	99.7
	420	227	205000	0.7	420	99.8
	427	228	205000	1.0	660	99.7
	435	228	205000	1.0	600	99.8

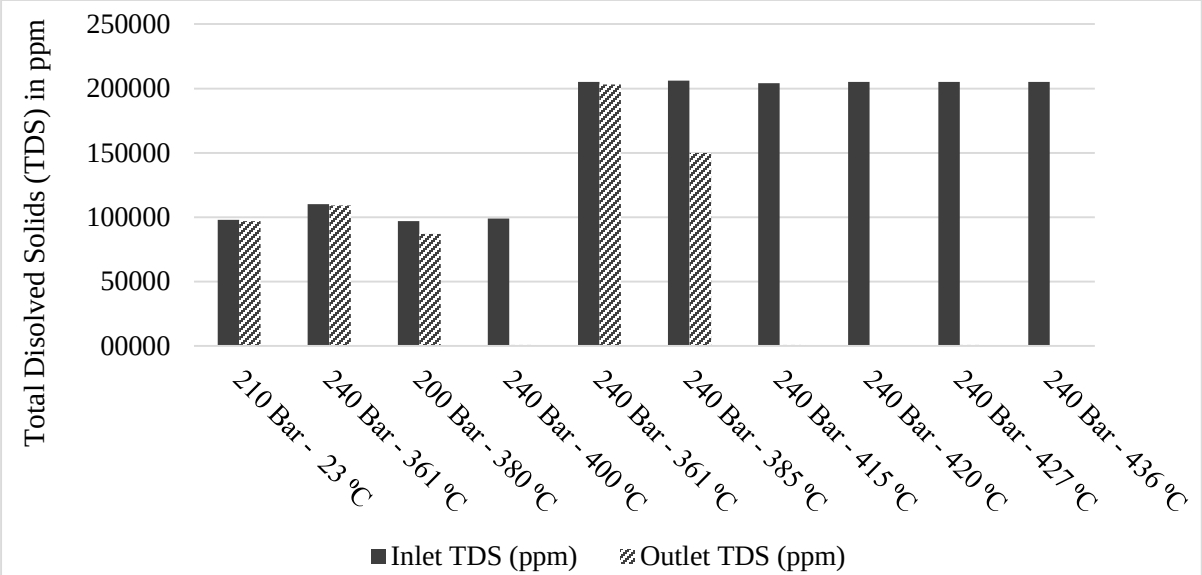

Figure 7. Inlet vs Outlet TDS in ppm.

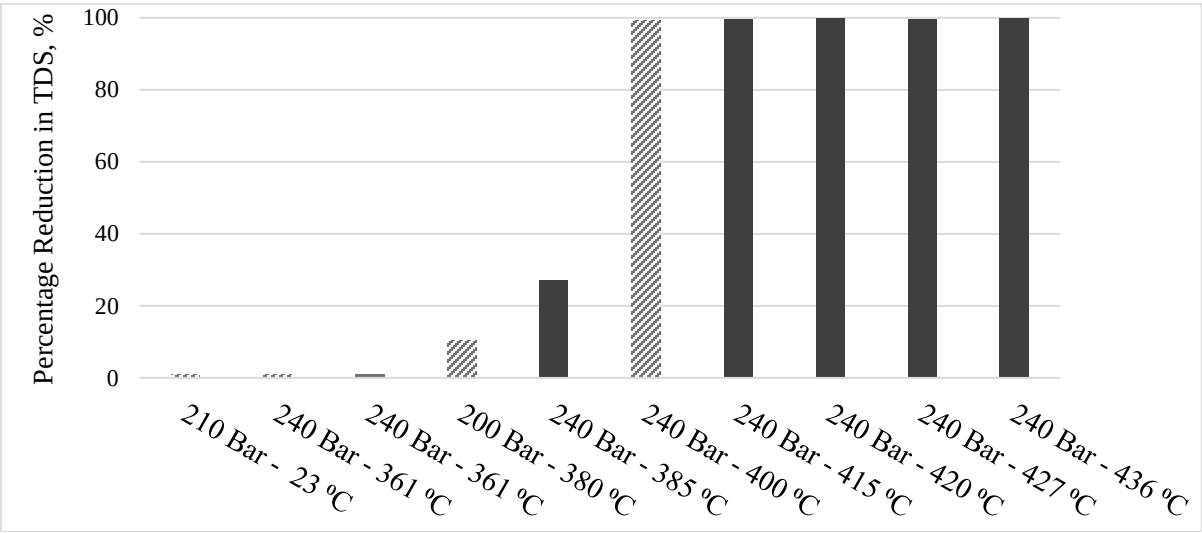

Figure 8. Percent reduction in TDS, under varied temperature, concentrations, and pressure conditions. (Pattern = 10% NaCl, Solid = 20% NaCl).

1.3.1. Energy Requirements for Salt Removal

To quantify the energy requirements for the SWEETR™ technology, new equipment was added and the preliminary operating procedures were slightly altered. The pre-heater was expanded to test higher flows and a theoretical study on the residence times was conducted using several parameters. This work and prior testing focused on developing operating temperature range and understanding the metrics to achieve desalination of the feed stream. This experimental work focused on investigating the energy input needed to achieve desalination.

To evaluate the power supplied, amp-meters with data logging capabilities were added to each of the power sources, This allowed for insitu measurement and display of the

energy input into the system. The heat input method was changed from the Watlow PID heater controllers, to Solid State Relay's (SSR) controlled by LabVIEW. This ensured heaters could be controlled with constant energy output for a given time, rather than the sinusoidal output provided by PID controllers.

Several tests were conducted to verify the highest operating temperatures that could be achieved while resulting in no desalination. Depending on the flow-rate, the optimal temperature range was found to be in-between 390°C and 395°C for the salt water feed. Operating at ~240 bar and the aforementioned temperature range resulted in no desalination, meaning the exit feed concentration was the same as the inlet feed concentration.

Once at this steady state, the heat source providing the extra energy for desalination would then be energized to the desired wattage and be held constant for 25 minutes. Under this methodology, the energy required to create the supercritical zone and achieve desalination could be isolated.

As the energy supplied for desalination was increased, the total amount of TDS removal also increased. Table 13 represents the preliminary energy requirements for the system, in order of rising energy requirements, for tests "I" through "L". Figure 9 shows the outlet concentrations versus time. The energy requirement is assuming no heat loss to the environment. The external heaters for the bulk fluids were held to a constant wattage, an assumption was made 100% transfer of energy from the extra heat supplied for desalination was transferred to the bulk fluid. The resulting energy requirements were positive, with a requirement of 310-339 MJ/m^3 to remove 73% and 82% of TDS respectively.

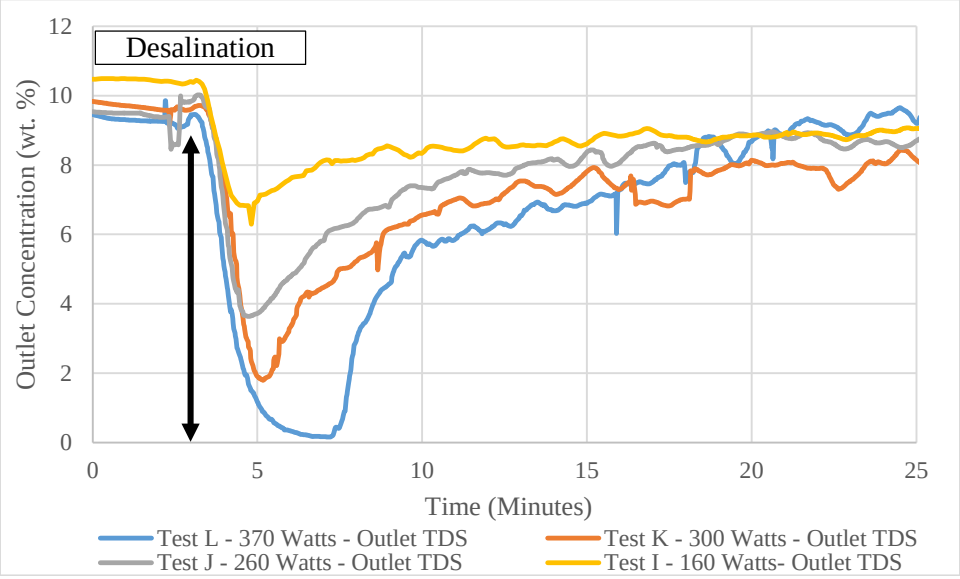

Figure 9. Outlet TDS vs Time.

Table 13. Energy Requirements for Desalination.

Test ID	Mass Flow Rate (g/min)	Vol. Flow (m^3/s)	Desalination Wattage	Energy Requirements (MJ/m^3)	Percent Reduction in TDS	Total TDS Removed	Salt Removed (grams)
I	44	7.480E-07	160	214	35%	37000	13
C	20.9	3.545E-07	110	310	73%	77000	56
A	27.8	4.726E-07	160	339	82%	86500	26
J	41	6.970E-07	260	373	66%	69000	21
G	25.3	4.301E-07	170	395	33%	35000	17
B	21.1	3.579E-07	153	428	79%	82900	38
K	40	6.800E-07	300	441	84%	88000	30
F	15	2.550E-07	115	451	67%	70000	19
J	45	7.650E-07	370	484	100%	105000	37
E	19.5	3.315E-07	170	513	71%	74100	29
H	22.5	3.825E-07	270	706	100%	105000	47

The temperatures are heavily dependent on a variety of factors such as pressures, flow rate, and insulation/heat loss to the environment. Thus maintaining a consistent steady state temperature across every test had proven to be a challenge. To mitigate this issue, the feed rate was monitored at the inlet as well as the exit, and the pump flow and pressured was adjusted as necessary prior to initiating the desalination tests. Still across several tests, there were variations in the starting and resulting temperatures. A summarized table of temperature profiles at key-points and other testing parameters is located in Table 14.

Table 14. Summarized Testing Parameters for Baseline Energy Testing.

Test Label	Pressure (Bar)	Freshwater Temperatures		Salt water Temperatures		Saltwater Temperature at Peak Removal		Peak Temperature		Avg. Flow Rate (grams/min)	Preheater/ Reactor Wattage	Addnl. Wattage/ Output %	Minimum Concentration at Outlet (wt. %)
A	244	Pre Heater	376	Pre Heater	394	Pre Heater	394	Desal Zone	412	27.8	1467/650	160 (39%)	1.85
		Lower Reactor	380	Lower Reactor	392	Lower Reactor	396	Lower Reactor	403				
		Reactor Exit	384	Reactor Exit	394	Reactor Exit	396						
B	245	Pre Heater	372	Pre Heater	394	Pre Heater	394	Desal Zone	407/397	21.05	1012/311	153/205 (39%/45 %)	2.21
		Lower Reactor	377	Lower Reactor	387	Lower Reactor	396	Lower Reactor	420/407				
		Reactor Exit	385	Reactor Exit	392	Reactor Exit	396						
C	244	Pre Heater	378	Pre Heater	394	Pre Heater	396	Desal Zone	412	20.85	1337/970	110 (32%)	2.8
		Lower Reactor	365	Lower Reactor	372	Lower Reactor	396	Lower Reactor	404				
		Reactor Exit	383	Reactor Exit	392	Reactor Exit	397						
D	240	Pre Heater	374	Pre Heater	NA	Pre Heater	393	Desal Zone	412	20.3	1050/395	125 (33%)	~0
		Lower Reactor	387	Lower Reactor	NA	Lower Reactor	403	Lower Reactor	403				
		Reactor Exit	393	Reactor Exit	NA	Reactor Exit	403						
E	240	Pre Heater	375	Pre Heater	394	Pre Heater	393	Desal Zone	414	19.5	1128/494	170 (39%)	3.09
		Lower Reactor	375	Lower Reactor	378	Lower Reactor	392	Lower Reactor	402				
		Reactor Exit	383	Reactor Exit	393	Reactor Exit	393						
F	244	Pre Heater	375	Pre Heater	390	Pre Heater	394	Desal Zone	410	15	760/612	115 (31.6%)	3.5
		Lower Reactor	372	Lower Reactor	380	Lower Reactor	395	Lower Reactor	403				
		Reactor Exit	380	Reactor Exit	393	Reactor Exit	395						
G	248	Pre Heater	374	Pre Heater	394	Pre Heater	393	Desal Zone	412	25.3	1025/310	170 (39%)	7
		Lower Reactor	374	Lower Reactor	375	Lower Reactor	395	Lower Reactor	402				
		Reactor Exit	377	Reactor Exit	385	Reactor Exit	395						
H	248	Pre Heater	377	Pre Heater	393	Pre Heater	393	Desal Zone	430	22.5	1118/384	270 (55%)	~0
		Lower Reactor	378	Lower Reactor	392	Lower Reactor	407	Lower Reactor	417				
		Reactor Exit	382	Reactor Exit	393	Reactor Exit	403						
I	248	Pre Heater	374	Pre Heater	394	Pre Heater	394	Desal Zone	410	44	1800/398	160 (39%)	6.8
		Lower Reactor	377	Lower Reactor	393	Lower Reactor	394	Lower Reactor	400				
		Desal Zone	377	Desal Zone	393	Desal Zone	405						
		Reactor Exit	381	Reactor Exit	394	Reactor Exit	395						
J	249	Pre Heater	x	Pre Heater	394	Pre Heater	394	Desal Zone	418	41	1754/388	260 (55%)	3.6
		Lower Reactor	x	Lower Reactor	394	Lower Reactor	397	Lower Reactor	405				
		Desal Zone	x	Desal Zone	393	Desal Zone	412						
		Reactor Exit	x	Reactor Exit	394	Reactor Exit	397						
K	250	Pre Heater	x	Pre Heater	395	Pre Heater	395	Desal Zone	424	40	2046/401	300 (67%)	1.7
		Lower Reactor	x	Lower Reactor	392	Lower Reactor	396	Lower Reactor	409				
		Desal Zone	x	Desal Zone	393	Desal Zone	414						
		Reactor Exit	x	Reactor Exit	393	Reactor Exit	396						
L	251	Pre Heater	x	Pre Heater	392	Pre Heater	396	Desal Zone	427	45	1987/377	370 (77%)	~0
		Lower Reactor	x	Lower Reactor	392	Lower Reactor	399	Lower Reactor	409				
		Desal Zone	x	Desal Zone	393	Desal Zone	412						
		Reactor Exit	x	Reactor Exit	394	Reactor Exit	400						

1.3.2. Solubility Modeling Work

Thermodynamic Modeling: Modeling was accomplished through the combined effort of several software packages – HSC, PHREEQC, and SoWAT. HSC is a thermochemical software with a versatile flowsheet simulation module. HSC is designed for various kinds of chemical reactions and equilibria calculations as well as process simulation, utilizing an extensive thermochemical database, which contains enthalpy (H), entropy (S), and heat capacity (C) data, for more than 28,000 chemical compounds. PHREEQC is an aqueous geochemical modeling software based on an ion-association aqueous model and has capabilities for speciation and saturation-index calculations, reaction-path and advective-transport calculations involving specified irreversible reactions, mixing of solutions, mineral and gas equilibria, surface- complexation reactions, and ion-exchange reactions.

The effect of temperature and pressure on salt concentrations was modeled using various equilibrium programs and can be validated by laboratory work. Some of the modeling software was used to help guide lab work (HSC, PHREEQC) does not have available data in the supercritical regime that can produce validated concentration models. Thus the evaluation of the effect of temperature and pressure on concentration modeled using HSC and PHREEQC in the pressure and temperature ranges of $25 \leq T \leq 450$ °C and $200 \leq P \leq 240$ bar and the results of this model during future testing could validated using laboratory data.

Preliminary modeling of a concentration curve in the subcritical regime using the equilibrium program HSC has produced interesting results. A sample of produced water obtained (Sample A1) and was used as a reference for the composition of produced water we are targeting to treat from the Bakken formation in western North Dakota. Table 15 shows the ionic constituents and concentrations in this produced water sample.

Table 15. Composition of produced water sample A1.

Constituents	Concentration (mg/L)	MW (g/mol)	mol/L	% mol
Ca^{+2}	22,400	40.1	0.559	0.00852
Mg^{+2}	1,430	24.3	0.0588	0.000897
Na^{+}	89,500	23.0	3.89	0.0593
K^{+}	7,400	39.1	0.189	0.00289
Li^{+}	60.0	6.94	0.00865	0.000132
Ba^{+2}	33.0	137	0.000240	3.66×10^{-6}
Fe^{+2}	152	55.8	0.00272	4.15×10^{-5}
Mn^{+2}	17.7	54.9	0.000322	4.91×10^{-6}
Sr^{+2}	1,540	87.6	0.0176	0.000268
Pb^{+2}	0.5082	207	2.45×10^{-6}	3.74×10^{-8}
Cl^{-}	190,000	35.5	5.35	0.0816
Br^{-}	816	79.9	0.0102	0.000156
SO_4^{-2}	197	96.1	0.00205	3.13×10^{-5}
F^{-}	33	19.0	0.00174	2.65×10^{-5}
HCO_3^{-}	61.0	61.0	0.00100	1.52×10^{-5}
NO_3^{-}	64.0	62.0	0.00103	1.57×10^{-5}
H_2O (L)	N/A	18.0	55.5	0.846

As seen in Table 15, calcium, sodium, and chlorine are the most prevalent ions present in this sample of produced water. Aspen was used to generate all possible salts from the present dissolved ions to be used in the equilibrium modeling. The Aspen-generated list of possible salt formations in this sample of produced water is seen in Table 16.

Table 16: Expected salt formations in a sample of Bakken produced water.

K_2SO_4	$Ca(NO_3)_2$	$MnBr_2$	$SrBr_2$
LiBr	NaCl	$MnCl_2$	$SrCl_2$
LiCl	Na_2SO_4	$MnSO_4$	$SrSO_4$
LiF	$KHCO_3$	$CaSO_4$	SrN_2O_6
$LiNO_3$	$FeBr_2$	NaF	$BaBr_2$
Li_2SO_4	$FeCl_2$	$PbCl_2$	$BaCl_2$
$MgBr_2$	$FeSO_4$	$NaHCO_3$	$Ba(NO_3)_2$
$MgCl_2$	KBr	$NaNO_3$	$BaSO_4$
$Mg(NO_3)_2$	KCl	$PbBr_2$	$CaBr_2$
CaF_2	KF	$Pb(NO_3)_2$	$CaCl_2$
$MgSO_4$	KNO_3	NaBr	

The Aspen-generated list of possible salt formations seen in Table 15 as well as the constituent compositions seen in Table 16 was used as input in the HSC Gibbs Energy Minimization (GEM) modeling performed. This sample was modeled at 200 bar, 220 bar, 230 bar, and 240 bar with temperatures being varied from 25°C → 450°C for each pressure setting. Preliminary results from HSC indicate that at these high pressures, a 40 bar difference has an insignificant effect on solubility. Figure 10 displays the solid phase composition of the produced water sample at 240 bar produced by HSC GEM. As Figure 11 shows, NaCl, $CaCl_2$, KCl, $SrCl_2$, and $MgCl_2$ are the most prevalent salts present in the solid phase and the temperatures where they expect to begin to precipitate. Figure 11 shows the results of the aqueous phase equilibrium from this same simulation.

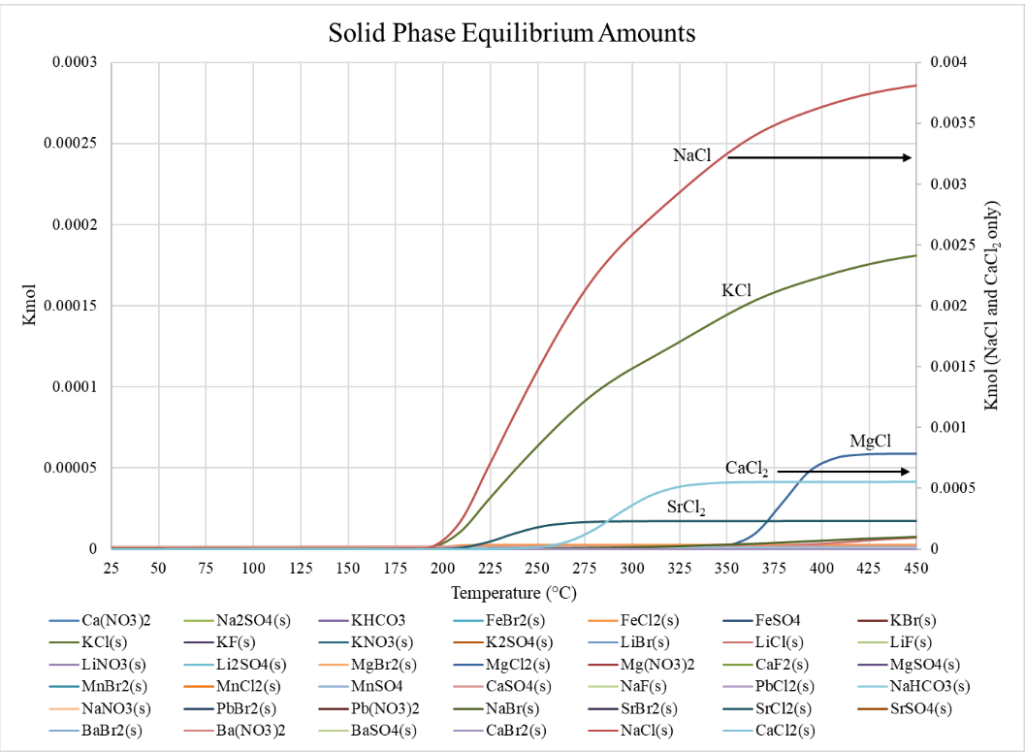

Figure 10. Solid phase equilibrium amounts at 240 bar.

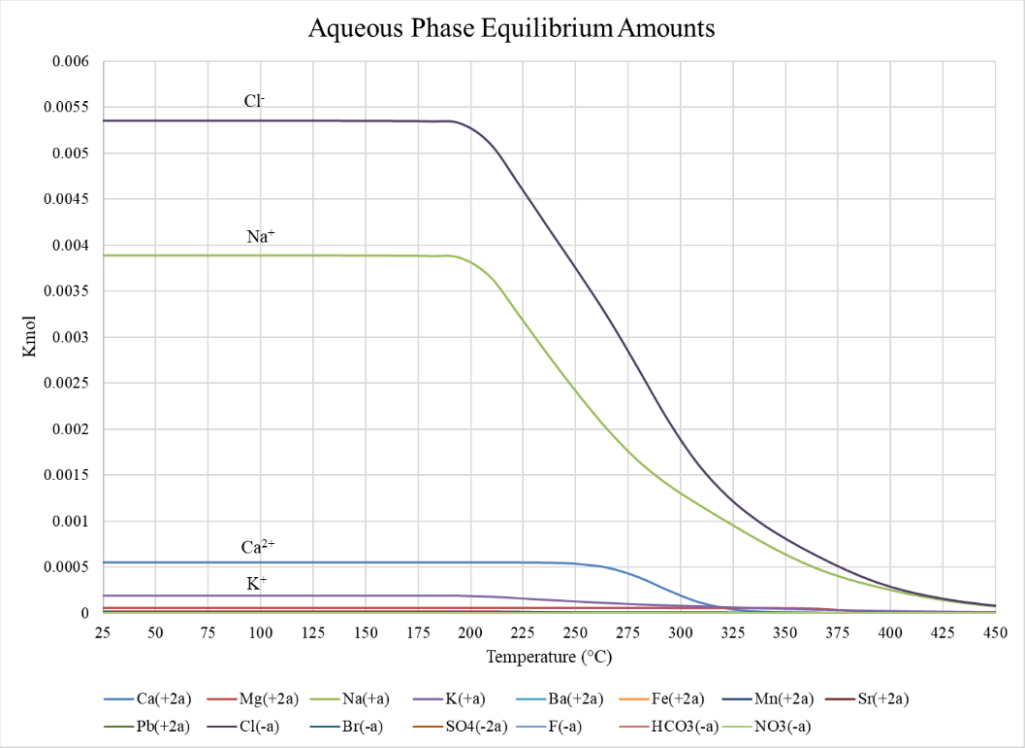

Figure 11. Aqueous phase equilibrium amounts at 240 bar.

It is suggested in Figure 11 that Na^+ and Cl^- solubility decrease drastically as temperatures approach 300°C. However, literature and previous test results suggest precipitation does not occur until higher temperatures, thus necessitating the use of the supercritical regime to adequately desalinate the produced water.

The validity of this equilibrium model is brought into question as temperatures exceed 200°C as this is where the model begins extrapolating its equilibrium data. Other models explored to date also appear to extrapolate data as the temperature approaches supercritical conditions. A goal for this project is to provide experimental data that can be used to compare and thus better validate this current model for future use. However, this and other models can still serve as a guide to salt precipitation behavior throughout this temperature domain.

PHREEQC Modeling: Building off of the HSC concentration modeling work presented in previous quarterly reports, a new modeling program was utilized to simulate produced water across the temperature range 25-450 °C at 240 bar. The geochemical program PHREEQC was used to simulate brines across the desired process conditions. Utilizing the same produced water sample illustrated in Table 15, a simulation of ion solubility across the temperature range 25-450 °C at 240 bar was generated in PHREEQC and the results are plotted in Figure 12.

It can be seen in Figure 12 that all ions experience reduced concentration as temperature is increased. As temperature nears the critical point of this solution (approximately 390 °C) the predicted concentration of Cl^-, Ca^{+2}, Na^+, and K^+ decreases rapidly as literature suggests will occur [23].

The gradual decrease in concentration for chloride, calcium, sodium, and potassium in the subcritical region (up to 365 °C) results in approximately 70% desalination from their initial concentrations. This desalination occurs across an approximately 350 °C temperature change. The desalination that occurs across the critical boundary of the solution is much more drastic considering the small temperature window the desalination occurs through.

Nearly 91% of the chloride, calcium, sodium, and potassium ions have precipitated out of solution once the solution passes its critical boundary (393.33 °C). This means that approximately 20% of the chloride, calcium, sodium, and potassium drop out of solution across a 28 °C temperature change. Similar behavior can be seen to exist for the less prevalent ions in solution as well.

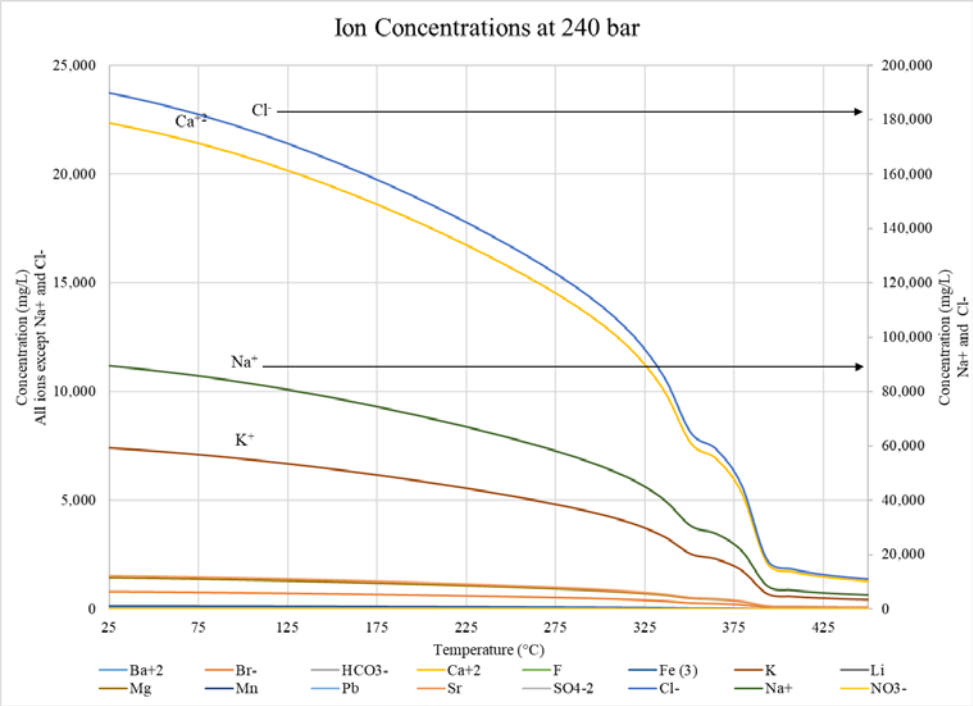

Figure 12. PHREEQC simulation output for produced water ion concentration at 240 bar.

There appears to be a small "pause" in desalination which occurs from approximately 350-360 °C for calcium, chloride, sodium, and potassium which does not have a behavioral explanation, thus it is likely a result of the model extrapolating between known datasets. The lack of available data across small temperature increments for multiple ions, especially near the critical point, leads to unexpected trends.

Discussion: A drawback of this model is the "pause" in desalination which occurs at 350-360 °C for all ions with no physical explanation beyond model error. This likely is due to inconsistencies between datasets which the model draws from for important species-specific parameters. The model draws primarily from a *pitzer.dat* dataset for its aqueous model which provides reasonable results across a wide range of conditions, however the model is limited in its species data availability as well as the data availability around the critical point. The lack of data around the critical point manifests itself in unrealistic solubility results such as the one experienced at 350-360°C.

SoWat Brine Property Model: The empirically-derived NaCl-H_2O solution property program SoWat was employed as a tool to simulate the solubility of a 10 wt% NaCl-H_2O solution from 25-450 °C at 240 bar. The program was developed using the empirical model developed by Thomas Driesner and written in C-code which operates on the DOS system [20, 21]. The ability to employ this model to accurately predict produced water solubilities along with other solution properties (density, specific heat, and enthalpy), utilizing the 'Trembly assumption', is an excellent resource for engineers working to develop a supercritical desalination technology.

Methods: The large temperature, pressure, and composition range which this model was developed to be valid across makes it an excellent candidate to be utilized in produced water solution property simulations, assuming the Trembley and Ogden assumption is employed and valid [22]. The Trembley and Ogden assumption, that a mixed salt system with NaCl as the primary constituent can be reasonably represented by a pure NaCl solution, is critical in employing this modeling program towards produced water solubility simulation. Without making this assumption, this model would not be applicable as it is derived for only a binary NaCl-H_2O solution. However, employing this assumption allows this model to be utilized in produced water solubility simulation as produced water's primary constituent is NaCl[3].

A 10 wt% solution was modeled across the temperature range 25-450 °C and held constant at 240 bar throughout the simulation. The simulation yielded the amount of phases present at each set of process conditions (temperature, pressure, and initial solution NaCl concentration) as well as the density, molar volume, heat capacity, and composition (X_{NaCl}) for each phase present. The results of the simulation were then tabulated into Microsoft Excel and plotted for evaluation.

Results: The SoWat predicted solution property results for a 10 wt% NaCl-H2O solution was reduced in Microsoft Excel and plotted for evaluation. The SoWat-predicted concentration curve for this solution can be seen in Figure 13.

It can be seen in Figure 13 that NaCL concentration decreases gradually as temperature is increased until approximately 390 °C, where the critical point of the solution is predicted to be. Once this temperature is surpassed, the concentration of NaCl decreases drastically. The concentration of NaCl decreases approximately 38% across the temperature range 25-389 °C from the initial concentration. Across the temperature range 389-400 °C, NaCl concentration decreases approximately 40% from the initial solution concentration alone.

This rapid decrease in concentration coincides with the phase change experienced at the critical point of the solution. This predicted concentration curve behavior shows strong agreement with what is expected based on literature [23]. Another rapid decrease in NaCl concentration can be seen at approximately 440 °C.

The rapid decrease in NaCl concentration at approximately 440 °C results in a roughly 10% decrease from the initial solution concentration. This behavior is the result of another predicted phase change. The predicted concentration along with the predicted phase changes can be seen in Figure 14.

[3] This is verified by the multiple produced water samples which have been sourced from the Bakken Formation in western North Dakota by this writer and analyzed by Standard Laboratories in Illinois.

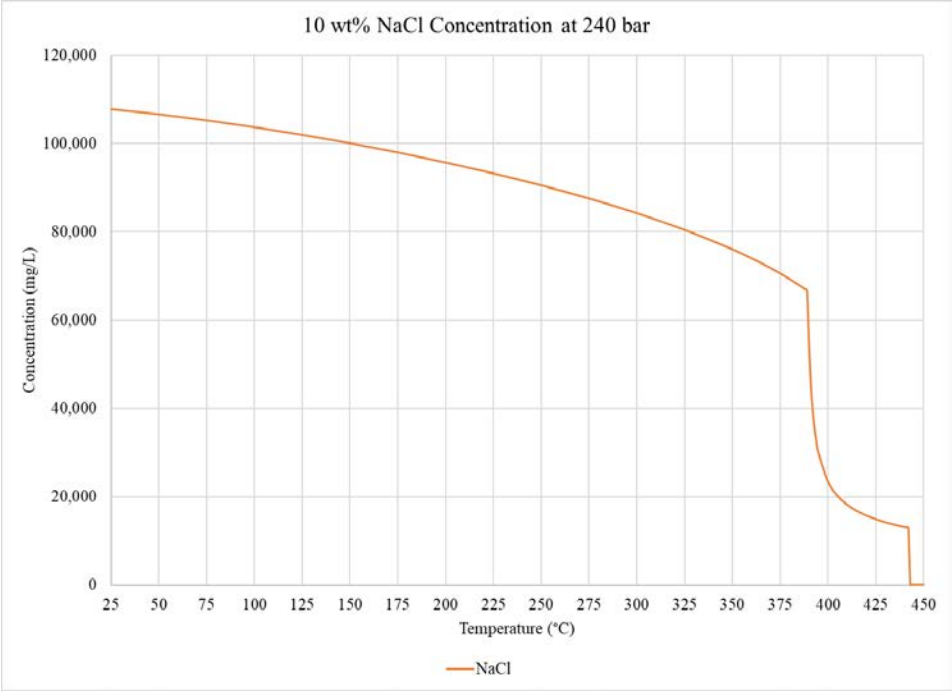

Figure 13. Driesner model-predicted NaCl solubility at 240 bar.

The predicted phases present as seen in Figure 14 coincide with key concentration behavior changes. The concentration of NaCl decreases gradually as temperature is increased throughout the liquid phase. Once the model predicted a two-phase system at approximately 390 °C the concentration of NaCl decreased drastically. NaCl concentration decreased drastically once more as the model predicted a new two-phase system to be in existence, a vapor and a solid phase.

One of the key differences between this model and others being evaluated (PHREEQC, and HSC) is the solution properties that the model predicts along with concentration. These solution properties are important to consider when developing an effective desalination system. The SoWat-predicted solution density curve as a function of temperature was constructed using a mass-weighted average of the densities for each present phase. This density curve can be seen in Figure 15.

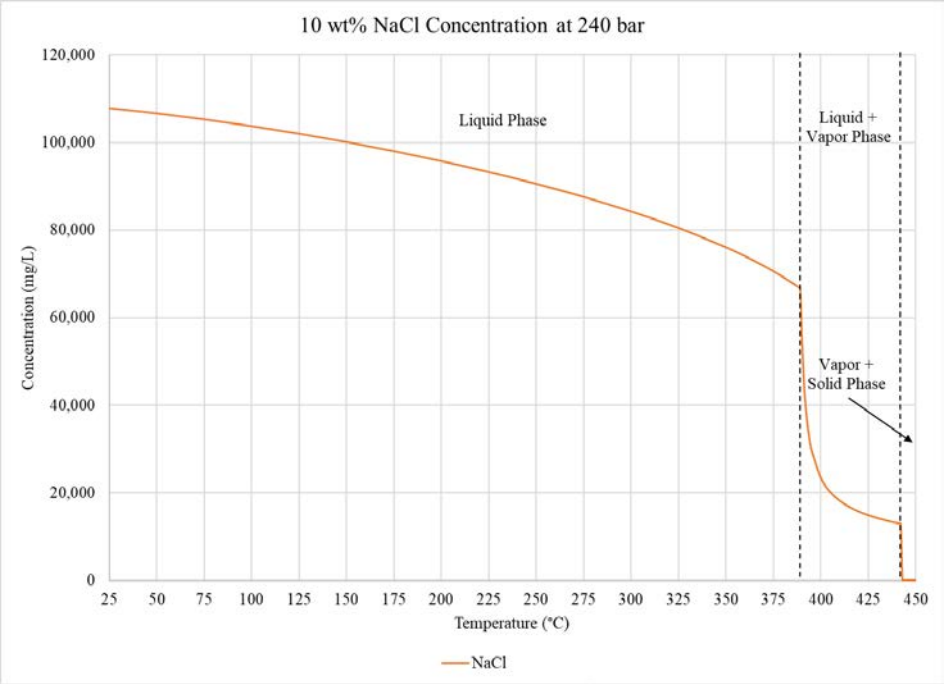

Figure 14: Driesner model predicted concentration with phases present.

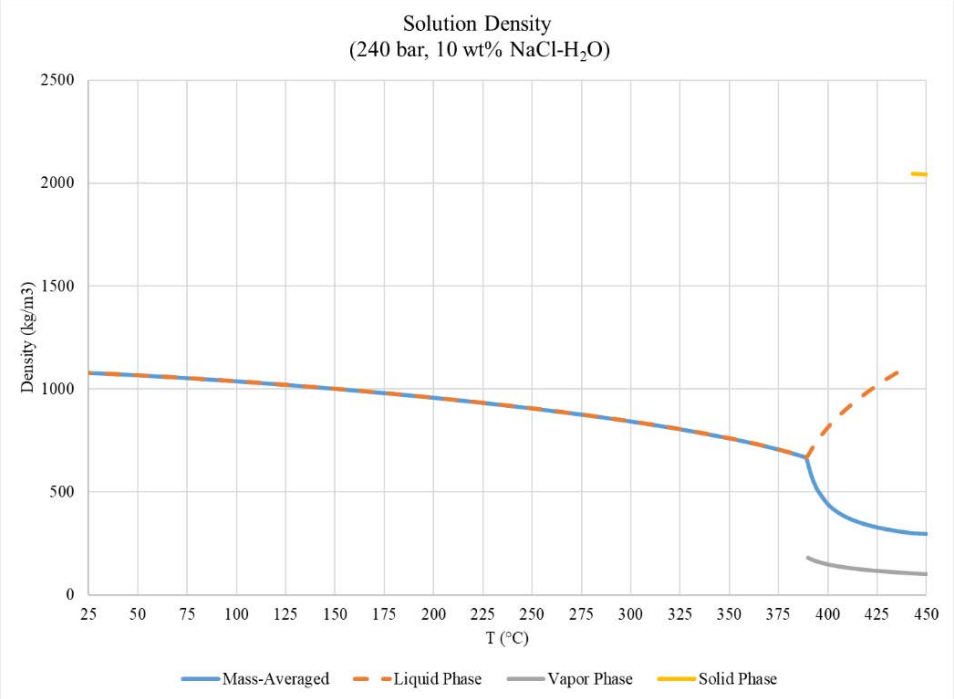

Figure 15: Driesner model-predicted solution mass averaged density as a function of temperature as well as each phase's predicted density.

The Driesner model-predicted density seen in Figure 15 follows the expected trend based on literature [20, 21, 23]. A slight decrease in solution density can be seen from 25-389 °C until the critical phase boundary is reached at 390 °C. Upon reaching this phase boundary, the density of the solution drops rapidly to approximately 300 kg/m^3. This

decrease in density is substantial compared to the initial starting solution density of 1080 kg/m^3. The decrease in density towards the vapor-like phase trend at these conditions is due to the vapor-like phase being the largest present phase at these conditions. The specific heat of the solution was also calculated and the mass-averaged specific heat as a function of temperature can be seen in Figure 16.

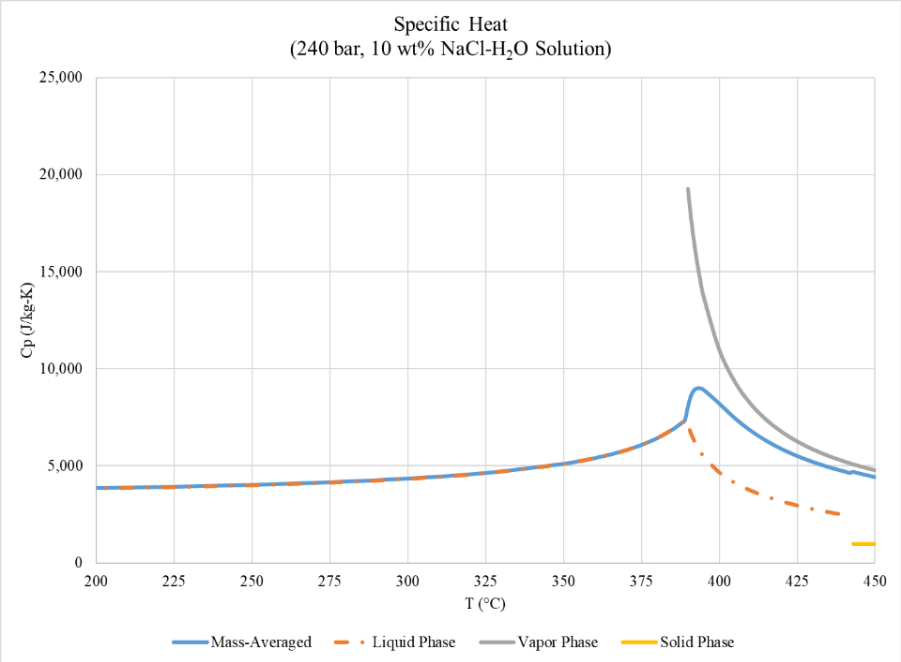

Figure 16. Driesner model-predicted mass-averaged specific heat as a function of temperature along with each phase's specific heat.

The predicted specific heat for the solution as a function of temperature varies significantly across the process temperature range simulated. The most significant change in the predicted solution's specific heat capacity comes as the critical phase is reached and surpassed at 390 °C. Once this solution reaches 390 °C the specific heat capacity increases to a maximum of 9,000 J/kg-K at 394 °C before decreasing to 4,400 J/kg-K at 450 °C. This trend follows the vapor-like phase trend at these conditions, likely as this phase is the largest present phase at these conditions.

Discussion: The Driesner model predicts valuable solution properties across the desired process conditions. The model's unique ability to accurately predict which phases are present at each set of process conditions as well as their respective properties (specific heat capacity, density, molar volume, and composition [X_{NaCl}]) increases the value of the model for use by engineers.

The rigorous validation method this model underwent throughout its formulation builds a high confidence level for users that the predicted properties are accurate. By utilizing a mass balance for dissolved NaCl, the complete solution phase composition can be determined with relative ease. Once the mass fraction for each phase present in solution is known, total solution properties can be determined on a mass-averaged basis as seen in Figure 16.

This model offers great value for engineers as important fluid properties like density as well as heat capacity can be determined with reasonable accuracy. The ability to know the specific heat capacity of a process fluid at desired process conditions allows for improved design characteristics with regards to heat transfer unit operations. The same rational is applied to density as true residence times in key unit operations are dependent on fluid density.

The only potential drawback of applying this model to produced water simulations is the use of the Trembley and Ogden assumption. The application of this model to multi-component brines such as produced water hinges on the application of the Trembley and Ogden assumption. If this assumption proves to not be as valid as previously thought, this model will not sufficiently predict fluid properties for a multi-component system as it does for a pure NaCl-H_2O solution.

Assuming the validity of the Trembly and Ogden assumption remains intact, the Driesner model successfully predicts fluid properties such as concentration, specific heat capacity, and density for any solution where the primary dissolved constituent is NaCl. This model accurately predicts behavior across key phase boundaries in the necessary high temperature and pressure process conditions likely to be employed in a supercritical water desalination system.

Model Comparison: Concentration curves produced by HSC, PHREEQC, and SoWat for a 3.2 wt% NaCl-H_2O solution were plotted and compared against each other as well as experimental data. The process conditions these simulations were run across were 25-450°C and 240 bar. 3.2 wt% NaCl was chosen as a concentration so the produced concentration curves were comparable to experimental data.

The SoWat predicted concentration curve served as the benchmark for model comparison as it was rigorously validated for binary NaCl-H2O solutions across these conditions [20, 21]. The comparison of the predicted NaCl concentration curves for each model can be seen in Figure 17.

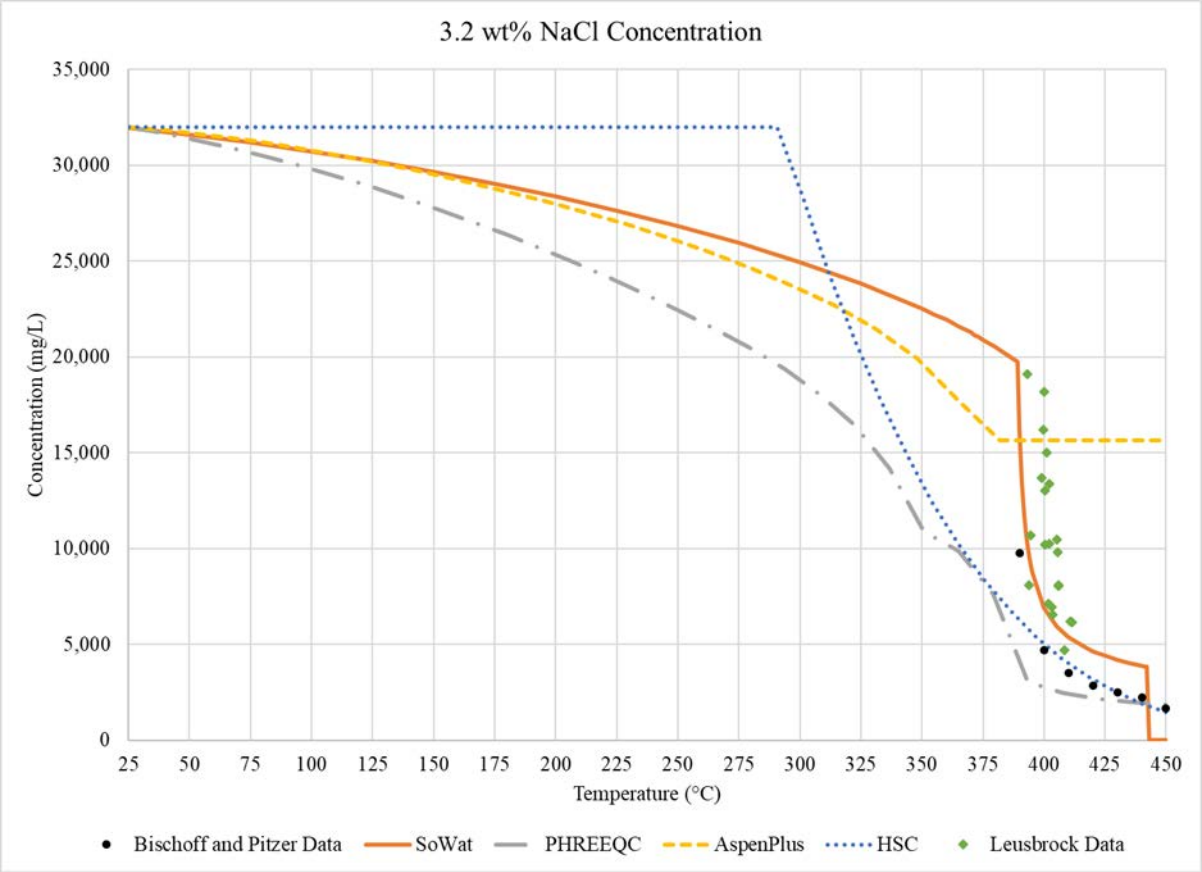

Figure 17. Comparison of predicted NaCl concentration curves from models to experimental data by Bischoff and Pitzer [24] as well as Leusbrock [23].

It can be seen in Figure 17 that the various models evaluated produce substantially different concentration curves for the same simulated solution. The HSC model drastically overestimates NaCl concentration from 25-300°C and underestimates NaCl concentration from 315-400°C. The PHREEQC concentration curve underestimates NaCl concentration across the entire temperature range of concern. This model shows moderate agreement with the Bischoff and Pitzer data from 400-450°C [24] however drastically deviates from the Leusbrock [23] data across the critical phase boundary from 380-400°C.

This model comparison shows the significant deviations in predicted concentration results produced by HSC, PHREEQC, and SoWat. Understanding how each model deviates from the actual NaCl concentration at various process conditions allows engineers to more confidently apply model results to process design. In this case, application of the SoWat model serves as an excellent resource for fluid properties across the desired process conditions in comparison to other commonly employed solution property models. Using the other models, especially near the supercritical region, will have significant impacts on the process model, and should be used with care if used to help size equipment and to develop mass and energy balances.

1.4. Produced water Pre-treatment approach

As a method of pretreatment, produced water samples were acquired and pH-adjusted for removal of valuable and problematic solids. The process of pH adjusting could be used as a pre-treatment step prior to desalination using the SWEETR™ technology. Four produced water samples were acquired from different well locations in the Bakken Formation, their composition is illustrated in Table 17, these samples were evaluated using this pH adjustment strategy.

Table 17. Summary of Composition of acquired produced water samples.

	Units	A1	B1	C1	D1
HCO_3	mg/L	0	12.2	4.9	20
Br	mg/L	861	694	285	848
Cl	mg/L	188000	178000	71400	159000
F	mg/L	0	0	0	0
Al	mg/L	0	0	0	0
Ca	mg/L	20100	12400	6240	15400
Fe	mg/L	44.8	87.6	53.7	112
K	mg/L	6830	4370	2040	5510
Mg	mg/L	1350	914	432	895
Mn	mg/L	18.6	9.02	5.37	105
Na	mg/L	84400	65100	29500	55200
Ba	mg/L	6460	6.32	3.7	9.43
Li	mg/L	60.8	16.2	7.35	20.9
Pb	mg/L	504	97.4	0.123	0.312
Sr	mg/L	1710	393	191	570
NO_3	mg/L	3525	0	0	0
SO_4	mg/L	278	258	226	169
Total TDS	mg/L	314,142	262,358	110,389	237,860

Produced water samples were adjusted to pH's 7, 8, 9, and 10 using NaOH. The focus of this pretreatment approach is to remove unstable materials from the feed solution. These materials could damage the process equipment, or lead to unexpected shutdown over time if continuously fed. The removal of iron-, sulfate, and silica-based materials are of particular interest. Once the desired pH is achieved it is maintained for 1 hour prior to the filtering out of precipitated solids. The solids are filtered (pore size: 2.5 μm), dried and analyzed using X-Ray Fluorescence (XRF) to determine their composition. It was determined an optimum pH for each of the produced water samples, this pH had shown significant removal of the Fe- contained in the solution. The reduction observed in each of the samples is summarized in Table 18 shown below.

Table 18: Maximum Reduction in Fe- observed under pH adjustment experiments.

Produced Water Sample	pH	Amount NaOH	Starting Fe- Concentration (mg/L)	Ending Fe- Concentration (mg/L)	% Reduction in Fe- from Starting Sample

		Added (g/L)			
A1	8	2.33	44.0	41.0	93%
B1	8	1.80	87.6	15.4	18%
C1	9	1.47	53.7	14.5	27%
D1	9	5.08	112	43.3	39%

FUTURE DIRECTIONS

The work reported here represents the end of work funded as a part of this project. The results obtained during the proof-of-concept testing demonstrate that the SWEETR™ concept is technically feasible and that supercritical water treatment is a viable option with strong merit for treating high salinity waters. The strategic design of the system provides the opportunity to localize the supercritical zone, which helps reduce the overall energy cost associated with the desalination process. The process can be tuned to remove only the amount of salts required to make the treated water "fit for purpose", providing further opportunities to minimize energy costs. The ability to destroy organic compounds associated with the water while simultaneously being able to desalinate makes SWEETR™ uniquely fitted for treating aqueous streams such as produced water from oil and gas extraction which contain small amounts of organics. Such mixed contaminant streams pose an extreme challenge for other treatment options. Future work will further develop the SWEETR™ technology to take it from the bench-scale to the pilot-scale, and ready the technology for commercial application.

2.0 REFERENCES

[1] López D., Trembly, J. Desalination of hypersaline brines with joule-heating and chemical pre-treatment: Conceptual design and economics. *Desalination* **2017,** *415*, pg. 49-57.

[2] Jiménez S., Micó M. M., Arnaldos M., Medina F., Contreras S. State of the art of produced water treatment. *Chemosphere* **2018**, *192*, pg. 186-208.

[3] Shrestha N., Chilkoor G., Wilder J., Gadhamshetty V., Stone JJ. Potential water resource impacts of hydraulic fracturing from unconventional oil production in the Bakken shale. *Water research* **2017,** *108*, pg. 1-24.

[4] Kurz B., Stepan D., Glazewski K., Stevens B., Doll T., Kovacevich J., Wocken C. A Review of Bakken Water Management Practices and Potential Outlook. **2016**.

[5] https://stateimpact.npr.org/pennsylvania/tag/deep-injection-well/ (Accessed 01/20/2019)

[6] https://www.eia.gov/todayinenergy/index.php?tg=steo%20(short-term%20energy%20outlook (Accessed 02/20/20)

[7] Rosenblum J., Nelson A., Ruyle B., Schultz M., Ryan J., Linden K. Temporal characterization of flowback and produced water quality from a hydraulically fractured oil and gas well. *Science of The Total Environment* **2017,** 596, pg. 369-377.

[8] Roberts D., Johnston E., Knott, N. Impacts of desalination plant discharges on the marine environment: a critical review of published studies. *Water Research* **2017**, 44 (18), pg. 5117–5128.

[9] https://www.thestar.com.my/news/world/2019/01/14/too-much-salt--water-desalination-plants-harm-environment-un/

[10] http://www.wcponline.com/2017/12/15/global-desalination-market-growth-continues (Accessed 01/21/19).

[11] *30th Worldwide Desalting Inventory*, published by GWI DesalData - International Desalination Association.

[12] Jones E., Qadir M., van Vliet M., Smakhtin V., Kang S. The state of desalination and brine production: A global outlook. *Science of the Total Environment* **2019**, 657, pg. 1343-1356.

[13] https://www.advisian.com/en/global-perspectives/the-cost-of-desalination (Accessed 01/18/2019).

[14] International Renewable Energy Agency (IRENA), *RENEWABLE ENERGY TECHNOLOGIES: COST ANALYSIS SERIES*. **June 2018**.

[15] Odu S., Van Der Ham A., Metz S., Kersten S. Design of a Process for Supercritical Water Desalination with Zero Liquid Discharge. *Industrial and Engineering Chemistry Research* **2015**, 54 (20), pg. 5527–5535.

[16] Hodes, M. Measurements and modeling of deposition rates from near-supercritical, aqueous, sodium sulfate and potassium sulfate solutions to a heated cylinder. *Massachusetts Institute of Technology* **1998**.

[17] Weast, R. Electrical conductivity of aqueous solutions. *CRC Handbook of Chemistry and Physics* **1989**, 70th Edition, CRC Press, Boca Raton, FL, p. D-221.

[18] Shnel O., and Novotny P. Concentrative properties of aqueous solutions Densities of Aqueous Solutions of Inorganic Substances **1985**, Elsevier, Amsterdam.

[19] Parsons, R. Manual Conductance Data (Emerson) Handbook of Electrochemical Constants **1959**. London, Butterworths Scientific Publications.

[20] Driesner T. and Heinrich C. The system H_2O-NaCl. Part I: Correlation formulae for phase relations in temperature-pressure-composition space from 0 to 1000°C, 0 to 5000 bar, and 0 to 1 X_{NaCl}. *Geochimica et Cosmochimica Acta* **2007**, 71, pg. 4880-4901.

[21] Driesner, T. The system H_2O-NaCl. Part II: Correlations for molar volume, enthalpy, and isobaric heat capacity from 0 to 1000°C, 1-5000 bar, and 0 to 1 X_{NaCl} *Geochimica et Cosmochimica Acta* **2007**, 71, pg. 4902-4919.

[22] Ogden D., and Trembly J. Desalination of hypersaline brines via Joule-heating: Experimental investigations and comparison of results to existing methods. *Desalination* **2017**, 424, pg. 149-158.

[23] Leusbrock I. Removal of inorganic compounds via supercritical water: fundamentals and applications. Groningen: Rijksuniversiteit Groningen, **2011**.

[24] Bischoff J. and Pitzer K. Liquid-vapor relations for the system NaCl-H_2O: summary of the P-T-x surface from 300° and 500°C. *American Journal of Science* **1989**, 289, pg. 217-248.

[25] Ding et al., Catalytic Supercritical Water Oxidation: Phenol Conversion and Product Selectivity. *Environment Science Technology* **1995**, 29, pg. 2748-2753.

[26] Krajnc M. and Levec J. Oxidation of Phenol over a Transition-Metal Oxide Catalyst in Supercritical Water. *American Chemical Society* **1997**, 36, pg. 3439- 3445.

[27] Wang et al. Catalytic performances of Ni-based catalysts on supercritical water gasification of phenol solution and coal-gasification wastewater*. International Journal of Hydrogen Energy* **2019**, 44, pg. 3470-3480.

[28] Rosenblum et al. Organic Chemical Characterization and Mass Balance of a Hydraulically Fractured Well: From Fracturing Fluid to Produced Water over 405 Days. *Environmental Science and Technology* **2017**, 51, pg. 14006-14015.

[29] Savage, P. Organic Chemical Reactions in Supercritical Water. *American Chemical Society* **1999**, 99, pg. 603-621.

PARTICPANTS & COLLABORATORS

Michael Mann Principal Investigator UND	Overall project management, broad direction of test planning and implementation, coordination with project partners, coordination with DOE PM.
Nicholas Dyrstad-Cincotta Research Engineer UND	Lead engineer for the design and operation of the experimental equipment. Assists principal investigator in coordinating schedules and reporting.
Ryder Shallbetter Research Engineer UND	Lead engineer for the process modeling and economic evaluation.
Joshua Oluwayomi Student UND	Provides hands-on help in performing experimental testing.
Sebastian Gardner Engineer UND	Primary focus is on theoretical and experimental modeling of salt solubility.

Olusegun Tomomewo Student UND	Combination of hands-on help performing experimental work and using experience as petroleum engineer in modeling salt solubility.
Teagan Nelson Research Engineer Envergex LLC	Assists in the design and operation of the experimental equipment, data analysis and report writing.
Srivats Srinivasachar Co- Principal Investigator Envergex LLC	Develops test strategies, interpret data, provide direction for the development of the process, assist in overall project management, develop commercialization plans
Hwanchul Cho Corporate Strategy Team Doosan Heavy Industries	Doosan lead on TEA

Acknowledgement: "This material is based upon work supported by the Department of Energy, Office of Energy Efficiency and Renewable Energy, Solar Energy Technologies Office, under Award Number DE-EE0008394.